RESEARCH

UDOT Keeping Utah Moving

Utah Department of Transportation - Research Division
4501 South 2700 West - P.O. Box 148410 - SLC,UT 84114-8410

Report No. UT-21.30

NON-DESTRUCTIVE EVALUATION AND NUMERICAL MODELING OF UNRATED INSTALLED CRASH BARRIERS

Prepared For:

Utah Department of Transportation
Research & Innovation Division

Final Report
June 2022

DISCLAIMER

The authors alone are responsible for the preparation and accuracy of the information, data, analysis, discussions, recommendations, and conclusions presented herein. The contents do not necessarily reflect the views, opinions, endorsements, or policies of the Utah Department of Transportation or the U.S. Department of Transportation. The Utah Department of Transportation makes no representation or warranty of any kind, and assumes no liability therefore.

ACKNOWLEDGMENTS

The authors acknowledge the Utah Department of Transportation (UDOT) for funding this research, and the following individuals from UDOT on the Technical Advisory Committee for helping to guide the research:

- Travis Jensen, UDOT Research Project Manager (consultant)
- Robert Dowell, UDOT Region 4 Traffic Operations Engineer
- Kendall Draney, UDOT Engineer for Maintenance
- Shawn Debenham, UDOT Roadside Safety Manager
- Glenn Blackwelder, UDOT Safety Operations Engineer
- Robert Miles, UDOT Director of Traffic & Safety
- Roland Stanger, FHWA Utah Division Safety & Operations Program Manager

TECHNICAL REPORT ABSTRACT

1. Report No. UT-21.30	2. Government Accession No. N/A	3. Recipient's Catalog No. N/A
4. Title and Subtitle NON-DESTRUCTIVE EVALUATION AND NUMERICAL MODELING OF UNRATED INSTALLED CRASH BARRIERS		5. Report Date June 2022 6. Performing Organization Code N/A
7. Author(s) Ashesh Pokhrel, Andrew Sorensen, Ph.D.		8. Performing Organization Report No. N/A
9. Performing Organization Name and Address Utah State University Department of Civil and Environmental Engineering 4110 Old Main Hill Logan, UT 84322-4110		10. Work Unit No. 73365 01D 11. Contract or Grant No. 20-8397
12. Sponsoring Agency Name and Address Utah Department of Transportation 4501 South 2700 West P.O. Box 148410 Salt Lake City, UT 84114-8410		13. Type of Report & Period Covered Final Oct 2019 to June 2022 14. Sponsoring Agency Code UT19.323

15. Supplementary Notes

Prepared in cooperation with the Utah Department of Transportation and the U.S. Department of Transportation, Federal Highway Administration

16. Abstract

Finite element models (FEM) for Midwest Guardrail System (MGS) and constant UDOT slope 42-in and 54-in cast-in-place (CIP) fixed barriers are created in LS-DYNA. The FEM of a Chevrolet Silverado pickup truck is used to perform a Test Level 3 (TL-3) crash simulation for the MGS. FEMs of a Ford 800 single unit truck (SUT) and a tractor-trailer are used, respectively, to perform TL-4 and TL-5 crash simulations for the 42-in and 54-in barriers. In the first phase of this report, these three barrier types are examined for their ability to contain and redirect the vehicles successfully using the commercial FEM software package LS-DYNA. The simulation results gave satisfactory results for the MGS in terms of structural adequacy (ability to contain and redirect) and for the 42-in and 54-in (1067 mm and 1372 mm) barriers in terms of structural adequacy and occupant risk factors. The flexible MGS barrier is able to reduce the speed of the crashing vehicle and redirect it while sustaining large deflection in the barrier section. In the case of rigid TL-4 and TL-5 barriers the vehicle is diverted into the same lane without overriding the barrier although permanent damage to the barrier and vehicles is observed. It is concluded that all three barrier types are safe and fulfill their functionality according to the Federal Highway Administration (FHWA) Manual for Assessing Safety Hardware (MASH) standards when analyzed using LS-DYNA.

17. Key Words MGS, UDOT 42 in (1067 mm) Constant Slope Barrier, UDOT 54 in (1372 mm) Constant Slope Barrier, MASH, FEM, LS-DYNA		18. Distribution Statement Not restricted. Available through: UDOT Research Division 4501 South 2700 West P.O. Box 148410 Salt Lake City, UT 84114-8410 www.udot.utah.gov/go/research		23. Registrant's Seal N/A
19. Security Classification (of this report) Unclassified	20. Security Classification (of this page) Unclassified	21. No. of Pages 74	22. Price N/A	

TABLE OF CONTENTS

LIST OF TABLES v
LIST OF FIGURES vi
UNIT CONVERSION FACTORS ix
LIST OF ACRONYMS x
EXECUTIVE SUMMARY xi
1. INTRODUCTION 1
1.1 Problem Statement 1
1.2 Objectives 4
1.3 Scope 5
1.4 Outline of Report 5
2. EVALUATION OF EXISTING LITERATURE 6
2.1 Introduction 6
2.2 Use of LS-DYNA to Test the Crashworthiness of Barriers 9
2.3 Modeling Techniques for Vehicle and Barrier Impacts 15
2.4 Comparison and Validation of FEM Results 18
2.5 Conclusion 20
3. EVALUATION PROCEDURE 21
4. TL-3 MASH EVALUATION OF MIDWEST GUARDRAIL SYSTEM (MGS) 22
4.1 FEM of MGS Barrier 22
4.2 FEM of 2007 Chevrolet Silverado Pickup Truck 23
4.3 Validity of TL-3 MGS Model 25
4.4 TL-3 Crash Simulation Time History of MGS Barrier 26
4.5 Structural Stability of MGS Barrier 28
4.6 Summary: MASH TL-3 Evaluation Criteria for MGS Barrier 30
5. MASH TL-4 EVALUATION OF UDOT 42-INCH CONSTANT SLOPE BARRIER 31
5.1 FEM of 42-in Barrier 31
5.2 Consistent Unit in LS DYNA 34
5.3 FEM of SUT 34
5.4 Validity of TL-4 Model 35
5.5 TL-4 Crash Simulation Time History Description 36

5.6 Occupant Risk Factors 41
5.7 Overturning Stability and Structural Damage of TL-4 Barrier 43
5.8 Summary: MASH TL-4 Evaluation Criteria for UDOT 42-in Barrier 44
6. TL-5 MASH EVALUATION OF UDOT 54-INCH CONSTANT SLOPE BARRIER 45
6.1 FEM of 54-in Barrier 45
6.2 FEM of Tractor-Trailer 47
6.3 Validity of TL-5 Model 49
6.4 TL-5 Crash Simulation Time History Description 50
6.5 Occupant Risk Factors 53
6.6 Overturning Stability and Structural Damage of TL-5 Barrier 55
6.7 Summary: MASH TL-5 Evaluation Criteria for UDOT 54-in Barrier 57
7. RESULTS AND CONCLUSION 59
REFERENCES 60

LIST OF TABLES

Table 2-1 Comparison of Test Procedures for MASH vs. NCHRP 350 7
Table 3-1 MASH Safety Evaluation Guidelines.....21
Table 4-1 MAST TL-3 Evaluation for MGS Barrier.....30
Table 5-1 Occupant Risk Factors Evaluation 42
Table 5-2 MASH TL-4 Evaluation Criteria for UDOT 42-in barrier.....44
Table 6-1 Occupant Risk Factors Evaluation 54
Table 6-2 MASH TL-5 Evaluation Criteria for UDOT 54-in Barrier 58

LIST OF FIGURES

Figure 1.1 Elevation View of MGS Installation 2
Figure 1.2 Section View of MGS Installation 3
Figure 1.3 UDOT 42-in Constant Slope Barrier 4
Figure 1.4 UDOT 54-in Constant Slope 4
Figure 2.1 Flow Chart for the Development/Evaluation of a Safety Feature 8
Figure 2.2 Time History Comparison of Real Crash Test and FEM (Itoh, 2007) 10
Figure 2.3 FEM vs Real Crash Test of an SUT (Esfahani, 2008) 12
Figure 2.4 Energy Balance in Simulation (Esfahani, 2008) 18
Figure 2.5 MASH Evaluation Procedure for a Barrier 19
Figure 4.1 MGS Barrier Full-Scale FEM 22
Figure 4.2 Different FEM Parts of MGS Barrier 23
Figure 4.3 FEM of MASH TL-3 Pickup Truck 24
Figure 4.4 MASH TL-3 Setup for MGS Barrier 24
Figure 4.5 Energy Balance Equation for Simulation of MGS 25
Figure 4.6 At t=0 s, Before Strike 26
Figure 4.7 At t=0.05 s, the First Wooden Block Fails 26
Figure 4.8 At t=0.205 s, Several Wooden Blocks Fail 27
Figure 4.9 At t=0.205 s, the Steel Posts That Come in Contact with Truck Fail 27
Figure 4.10 At t=0.355 s, the Vehicle Starts to Divert Back into the Roadway 27
Figure 4.11 At t=0.535 s, the Front Wheel of Vehicle Moves Away from Barrier While Diverting Back 27
Figure 4.12 At t=0.7 s, the Vehicle is Diverted While the W-Beam Failed from the Posts 28
Figure 4.13 Failure Between the W-Beam, Wooden Block and Post 29
Figure 4.14 Resultant Velocity of the Truck after Impact with MGS Barrier 29
Figure 4.15 Maximum Displacement of W-Beam 30
Figure 5.1 Cross-Section View of 42-in (1067 mm) Barrier 31
Figure 5.2 Isometric View of 42-in (1067 mm) Barrier 31
Figure 5.3 FEM of Barrier, Base and Ground 32
Figure 5.4 FEM of Dowel Bars and Base 33
Figure 5.5 Barrier Reinforcement FEM 33

Figure 5.6 Stress-Strain Curve for Reinforcement Bars 33
Figure 5.7 FEM F800 SUT 35
Figure 5.8 FEM Truck and TL-4 Barrier 35
Figure 5.9 Energy Balance Equation for Simulation of TL-4 42-in (1067 mm) Barrier 35
Figure 5.10 At t=0 s, before Impact 37
Figure 5.11 At t=0.09 s, Frontal Crush of the Vehicle is Observed 37
Figure 5.12 At t=0.16 s, the Front Part of Vehicle Starts to Redirect 37
Figure 5.13 At t=0.2 s, the Trailer Overrides the Barrier 37
Figure 5.14 At t=0.28 s, the Back Tires Come in Contact with the Barrier 38
Figure 5.15 At t=0.32 s, the Back Tires Ride the Barrier and Slide against it 38
Figure 5.16 At t= 0.42 s, the Unstiffened Parts of Truck Fail and Truck Becomes Unstable 38
Figure 5.17 At t=0.65 s, Both Front and Back Tires Slide against the Barrier 38
Figure 5.18 At t=0.76 s, the SUT Leans against the Barrier 39
Figure 5.19 At t=0.81 s, the SUT Body Slides against the Barrier 39
Figure 5.20 At t=0.95s, the SUT Continues Sliding along the Barrier 39
Figure 5.21 At t=1.1s, the SUT Continues Sliding along the Barrier 39
Figure 5.22 At t=1.22 s, the Front Wheels are in the Air While the SUT is Being Directed 40
Figure 5.23 At t=1.31 s, the Truck is Diverted with Wheels Down 40
Figure 5.24 At t=1.52 s, the SUT is Directed away from the Barrier Completely; Significant Damage is Observed 40
Figure 5.25 At t=2.2 s, Simulation Ends 40
Figure 5.26 Accelerometer Location to Measure Different Risk Factors 41
Figure 5.27 TL-4 Roll Rate 42
Figure 5.28 TL-4 Pitch Rate 42
Figure 5.29 Damage of 42-in Barrier 43
Figure 5.30 Displacement of Barrier 43
Figure 6.1 Cross-Section View of 54-in (1372 mm) Barrier 45
Figure 6.2 Isometric View of 54-in (1372 mm) Barrier 45
Figure 6.3 FEM of Barrier, Base and Ground 46
Figure 6.4 FEM of Dowel Bars in PCCP Base 46
Figure 6.5 FEM of 54-in (1372 mm) Barrier Reinforcement 46

Figure 6.6 Sleeper-Cab Tractor FEM 47
Figure 6.7 Trailer FEM 48
Figure 6.8 Full FEM of Tractor-Trailer 48
Figure 6.9 Tractor, Trailer and Load Together 48
Figure 6.10 Joint Between Fifth Mechanical Wheel and Kingpin 49
Figure 6.11 Connection Between Tractor and Trailer 49
Figure 6.12 Energy Balance Equation for Simulation of TL-5 54-inch Barrier 49
Figure 6.14 At t=0.07 s, Immediately after Impact, Crushing of Front Part 50
Figure 6.13 At t=0 s, Prior to Impact 50
Figure 6.15 At t=0.13 s, after Impact the Tractor Starts to Redirect 51
Figure 6.16 At t= 0.29 s, Contact between the Trailer and Barrier 51
Figure 6.17 At t=0.38 s, Redirection of Trailer after the Impact 51
Figure 6.18 At t= 0.52 s, after Impact, No Contact with the Barrier 51
Figure 6.19 At t=0.75 s, Contact of Rear Part of Trailer with Barrier 52
Figure 6.20 At t=0.83 s, Trailer Comes in Contact and Slides along Barrier 52
Figure 6.21 At t=0.9 s, Tractor-Trailer Diverts from the Barrier 52
Figure 6.22 At t=1.03 s, Front Part of Trailer Comes in Contact again with Barrier 52
Figure 6.23 At t=1.2 s, Tractor-Trailer is Completely Diverted from the Barrier 53
Figure 6.24 Accelerometer Mounted in Tractor 53
Figure 6.25 TL-5 Roll Rate 54
Figure 6.26 TL-5 Pitch Rate 55
Figure 6.27 At t=0.11s Tractor Comes in Contact with the Barrier 55
Figure 6.28 At t=0.33 s Trailer is Rebounded from the Barrier 56
Figure 6.29 Damage of Concrete Elements 56
Figure 6.30 Damage in Reinforcement Elements 56
Figure 6.31 Nodal Displacement History of Concrete Node 57
Figure 6.32 Vertical Displacement of Barrier 57

UNIT CONVERSION FACTORS

SI* (MODERN METRIC) CONVERSION FACTORS

APPROXIMATE CONVERSIONS TO SI UNITS

Symbol	When You Know	Multiply By	To Find	Symbol
		LENGTH		
in	inches	25.4	millimeters	mm
ft	feet	0.305	meters	m
yd	yards	0.914	meters	m
mi	miles	1.61	kilometers	km
		AREA		
in^2	square inches	645.2	square millimeters	mm^2
ft^2	square feet	0.093	square meters	m^2
yd^2	square yard	0.836	square meters	m^2
ac	acres	0.405	hectares	ha
mi^2	square miles	2.59	square kilometers	km^2
		VOLUME		
fl oz	fluid ounces	29.57	milliliters	mL
gal	gallons	3.785	liters	L
ft^3	cubic feet	0.028	cubic meters	m^3
yd^3	cubic yards	0.765	cubic meters	m^3
	NOTE: volumes greater than 1000 L shall be shown in m^3			
		MASS		
oz	ounces	28.35	grams	g
lb	pounds	0.454	kilograms	kg
T	short tons (2000 lb)	0.907	megagrams (or "metric ton")	Mg (or "t")
		TEMPERATURE (exact degrees)		
°F	Fahrenheit	5 (F-32)/9 or (F-32)/1.8	Celsius	°C
		ILLUMINATION		
fc	foot-candles	10.76	lux	lx
fl	foot-Lamberts	3.426	$candela/m^2$	cd/m^2
		FORCE and PRESSURE or STRESS		
lbf	poundforce	4.45	newtons	N
lbf/in^2	poundforce per square inch	6.89	kilopascals	kPa

APPROXIMATE CONVERSIONS FROM SI UNITS

Symbol	When You Know	Multiply By	To Find	Symbol
		LENGTH		
mm	millimeters	0.039	inches	in
m	meters	3.28	feet	ft
m	meters	1.09	yards	yd
km	kilometers	0.621	miles	mi
		AREA		
mm^2	square millimeters	0.0016	square inches	in^2
m^2	square meters	10.764	square feet	ft^2
m^2	square meters	1.195	square yards	yd^2
ha	hectares	2.47	acres	ac
km^2	square kilometers	0.386	square miles	mi^2
		VOLUME		
mL	milliliters	0.034	fluid ounces	fl oz
L	liters	0.264	gallons	gal
m^3	cubic meters	35.314	cubic feet	ft^3
m^3	cubic meters	1.307	cubic yards	yd^3
		MASS		
g	grams	0.035	ounces	oz
kg	kilograms	2.202	pounds	lb
Mg (or "t")	megagrams (or "metric ton")	1.103	short tons (2000 lb)	T
		TEMPERATURE (exact degrees)		
°C	Celsius	1.8C+32	Fahrenheit	°F
		ILLUMINATION		
lx	lux	0.0929	foot-candles	fc
cd/m^2	$candela/m^2$	0.2919	foot-Lamberts	fl
		FORCE and PRESSURE or STRESS		
N	newtons	0.225	poundforce	lbf
kPa	kilopascals	0.145	poundforce per square inch	lbf/in^2

*SI is the symbol for the International System of Units. (Adapted from FHWA report template, Revised March 2003)

LIST OF ACRONYMS

AASHTO	American Association of State Highway and Transportation Officials
ANOVA	Analysis of Variance
CG	Center of Gravity
CIP	Cast in Place
FEM	Finite Element Modeling
FHWA	Federal Highway Administration
GWU	George Washington University
HGV	Heavy Goods Vehicle
MARA	Maximum Absolute Roll Angle
MASH	Manual for Assessing Safety Hardware
MGS	Midwest Guardrail System
MPC	Magnitude-Phase-Comprehensive
MWRSF	Midwest Roadside Safety Facility
NCHRP	National Cooperative Highway Research Program
NJ	New Jersey
OIV	Occupant Impact Velocity
ORA	Occupant Ride Down Acceleration
ORNL	Oak Ridge National Laboratory
PCB	Portable Concrete Barrier
PCCP	Portland Cement Concrete Pavement
RBF	Radial Basis Function
RSVVP	Roadside Safety Verification and Validation Program
SUT	Single Unit Truck
TL-3	Test Level Three
TL-4	Test Level Four
TL-5	Test Level Five
UDOT	Utah Department of Transportation
YLM	Yield Line Method

EXECUTIVE SUMMARY

Finite element models (FEM) for Midwest Guardrail System (MGS), constant slope 42-in and 54-in (1067 mm & 1372 mm) barriers are created in LS-DYNA. The FEM of a Chevrolet Silverado pickup truck for Manual for Assessing Safety Hardware (MASH) Test Level 3 (TL-3), a Ford 800 Single Unit Truck for MASH Test Level 4 (TL-4), and a Tractor-Trailer for MASH Test Level 5 (TL-5) are used to perform crash simulation for each barrier type. In this report the 42-in and 54-in (1067 mm and 1372 mm) constant slope barrier are examined for their ability to contain and redirect the vehicles successfully using the commercial FEM software package LS-DYNA. The simulation results gave satisfactory results for the MGS in terms of structural adequacy and for the 42-in and 55-in (1067 mm & 1372 mm) barriers in terms of structural adequacy (ability to contain and redirect) and occupant risk factors. The flexible MGS barrier is able to reduce the speed of the crashing vehicle and redirect it while sustaining large deflection in the barrier section. In the case of rigid TL-4 and TL-5 barriers, the vehicle is diverted into the same lane without overriding the barrier although permanent damage to the barrier and vehicles is observed. Small overturning moment and localized structural damage in concrete was observed. It is concluded that the MGS barrier and the 42-in and 54-in (1067 mm and 1372 mm) constant slope barriers are safe and fulfill their functionality according to Federal Highway Administration (FHWA) MASH standards when analyzed using LS-DYNA.

1. INTRODUCTION

1.1 Problem Statement

The Utah Department of Transportation (UDOT) has approximately 3.6 billion dollars' worth of crash barriers currently in service. Crash barriers are currently rated for effectiveness using the American Association of State Highway and Transportation Officials (AASHTO) Manual for Assessing Safety Hardware (MASH). Prior to this, crash barriers were rated according to National Cooperative Highway Research Program Report Number 350 (NCHRP Report 350) criteria. MASH specifies different testing criteria that crash barriers or guardrail must pass in order to be rated at certain levels. The basic level, or Test Level 3 (TL-3), that longitudinal barriers must support is, for example, 2420 lb to 5000 lb (1100 kg to 2270 kg) vehicles traveling at 62 mph (100 km/h) at a nominal impact angle of 25° (as well as other impact scenarios). The previous NCHRP report 350 criteria required an 1890 lb to 4409 lb (820 kg to 2000 kg) vehicle traveling at 62 mph (100 km/h) at a nominal impact angle of 20°. Crash barriers are certified according to MASH standards prior to installation and new barrier designs are certified by the Federal Highway Administration (FHWA). However, a number of crash barriers currently in service around the state pre-date the new MASH rating system and as such, UDOT does not have a definitive knowledge of the impact resistance of these barriers. Additionally, FHWA has recently announced plans to discontinue its practice of certifying crash barriers. These factors have necessitated a local ability to evaluate installed crash barriers non-destructively.

Longitudinal barriers prevent the entry of vehicles into opposite lanes and prevent loss of life and property. Barriers are either rigid or flexible. Rigid barriers produce higher vehicle decelerations and prevent any lateral deflections while flexible barriers produce lower deceleration and allow large lateral deflections. Barriers designed and tested for higher test levels are generally used on high-speed, high-volume roads such as freeways or interstates (AASHTO, 2016).

To protect the road users from hazards, UDOT uses Midwest Guardrail System (MGS) on its highway systems for a number of applications like adjacent to steep slopes and high flare

rates. MGS barriers (Figure 1.1, Figure 1.2) are the upgrade to the standard W-beam guardrail, commonly known as G4 W-beam guardrail, which is widely used in the highway systems in the United States. Due to the increase in the center of gravity of vehicles used in recent years, the G4 W-beam is close to reaching its performance limits. The major difference between G4 W-beam guardrail and the MGS is the rail height, which is 27 in (386 mm) in G4 and 31 in (787 mm) in MGS. Similarly, the W-beam splices from the posts are moved to the mid-span between the posts and the wooden block depth is 12 in (305 mm) in MGS as compared to 8 in (203 mm) in G4. MGS barriers use W6x9 steel posts or 6 in x 8 in (152 mm x 203 mm) wood posts and are placed 6 ft (1.83 m) apart. MGS has satisfied the MASH TL-3 criteria and has been experimentally validated (Faller et al., 2004; Sicking, Reid, & Rohde, 2002).

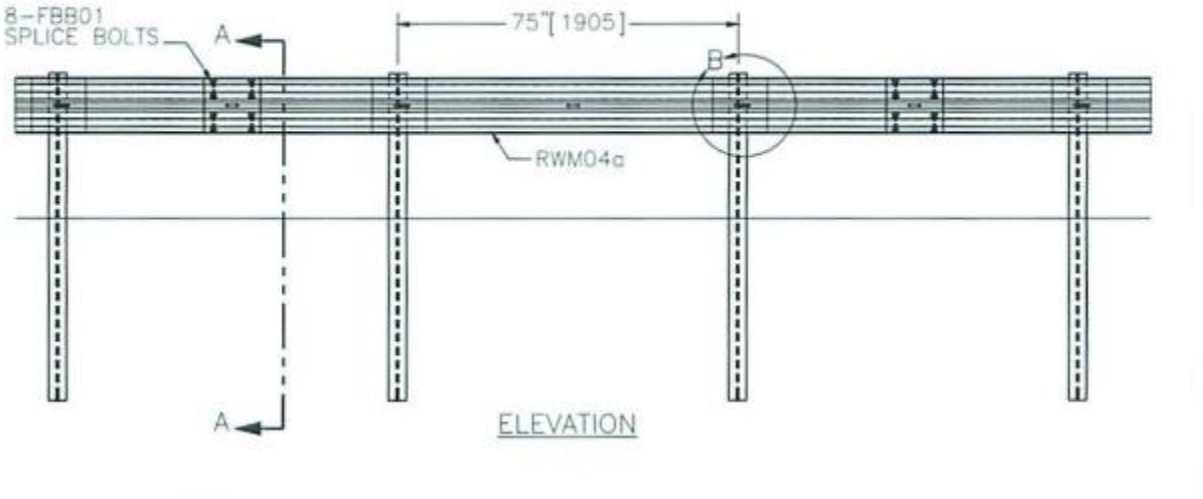

Figure 1.1 Elevation View of MGS Installation

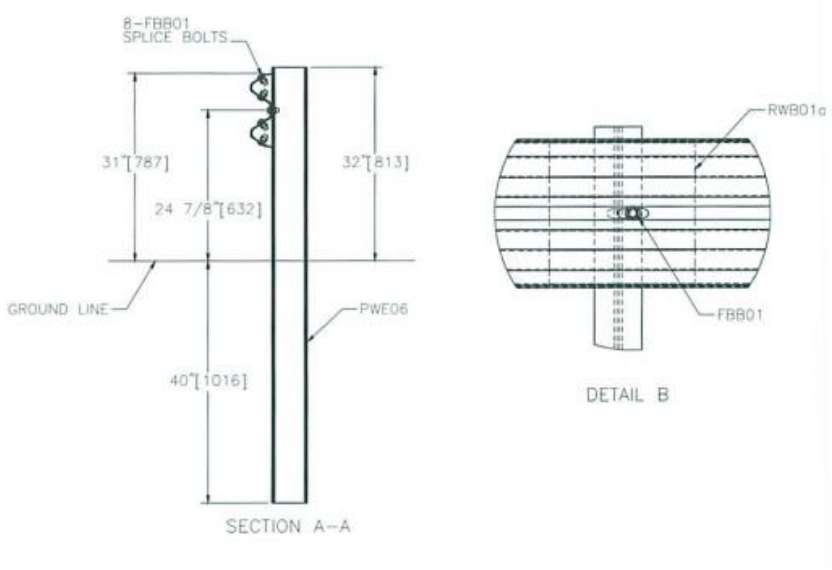

Figure 1.2 Section View of MGS Installation

UDOT also uses cast-in-place (CIP) constant slope barriers such as the 42-in (1067 mm) (Figure 1.3) and the 54-in (1372 mm) tall constant slope barrier (Figure 1.4) in various configurations and reinforcement details to satisfy different MASH test levels. In this study the barriers are constructed as fixed barriers in Portland Cement Concrete Pavement (PCCP) and are fixed to the concrete pavement using dowel bars. The 42-in (1067 mm) barrier is studied for MASH TL-4 application and the 54-in (1372 mm) barrier is studied for MASH TL-5 application.

All new barriers and hardware to be installed on highways need to pass MASH safety standards as per UDOT's policy. MASH has prescribed the use of finite element software, mainly LS-DYNA, as a tool to analyze the safety features to be implemented on highways. LS-DYNA can simulate the exact crash scenario for different test levels and provide researchers and designers with prior performance before carrying out physical crash testing. The developed models can be validated using previously published literature on other crash barriers using similar modeling techniques.

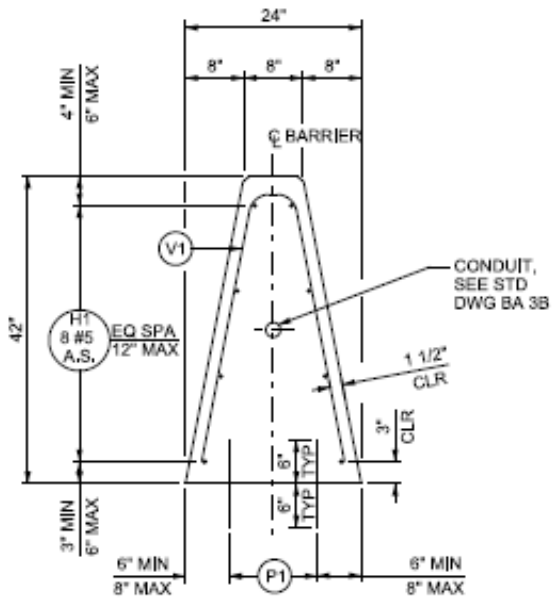

Figure 1.3 UDOT 42-in Constant Slope Barrier

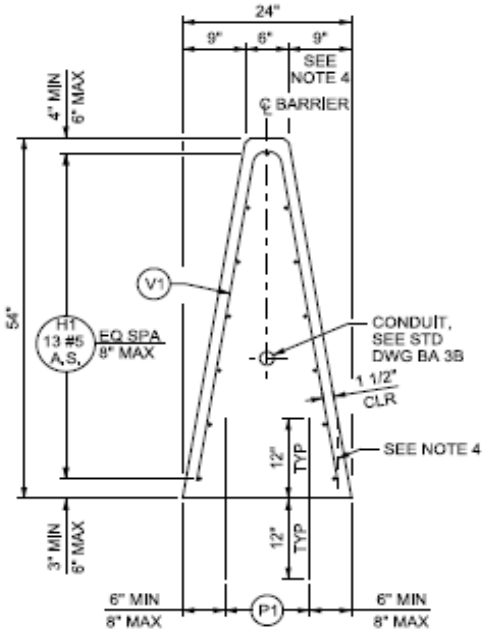

Figure 1.4 UDOT 54-in Constant Slope Barrier

This project provides a number of benefits to UDOT. First, it develops a finite-element model- (FEM) development procedure where new barriers can be evaluated prior to carrying out a fully constructed testing regime. This has the potential for significant cost savings to UDOT especially as the latest MASH standards require that a barrier pass all testing regimens without failure or the entire testing procedure must be started again at the beginning. Second, the developed modeling procedure provides a framework for estimating the MASH rating for crash barrier where the rating is currently unknown. This will provide decision makers within the UDOT Traffic and Safety Division with information needed to properly manage these assets.

1.2 Objectives

The primary objective of this research project is to develop a validated numerical modeling and testing procedure to approximate the MASH rating of UDOT crash barriers using

FEM techniques. A secondary objective of this research project is to estimate the MASH rating of three existing UDOT crash barriers.

1.3 Scope

The following tasks are carried out in this project:

1. Develop an overview of current practices in both physical testing and numerical modeling of crash barriers.
2. Develop a framework for FEM of barriers including the collection of previously developed vehicle FEMs.
3. Develop three validated FEMs for the MGS 42-in (1067 mm) and 54-in (1372 mm) constant slope barriers.
4. Use the validated FEMs to simulate MASH testing criteria in order to determine an approximate rating for the two unknown barriers.
5. Prepare a final report based on the results of the testing and MASH simulations.

1.4 Outline of Report

This report is divided into the following chapters:

1. Introduction
2. Evaluation of Existing Literature
3. Evaluation Procedure
4. TL-3 MASH Evaluation of Midwest Guardrail System (MGS)
5. TL-4 MASH Evaluation of 42-in (1067 mm) Constant Slope Barrier
6. TL-5 MASH Evaluation of 54-in (1372 mm) Constant Slope Barrier
7. Summary of Conclusions

2. EVALUATION OF EXISTING LITERATURE

2.1 Introduction

Safety barriers prevent the intrusion of vehicles into other lanes or into highway work/construction zones. Fixed or Portable Concrete Barriers (PCB) are one of the most widely used structures for this purpose. Barriers are available in various shapes, sizes, length and connection details. Along with the portable barriers like New Jersey (NJ)-shape and F-shape, CIP or fixed barriers like single slope barriers and vertical slope barriers are some of the most common median barriers. The shape of the barrier plays an important role in the vehicle dynamics after impact. Barrier geometries have been constantly updated since being introduced to highways. F-shape barriers can be taken as one of the best examples because they are an updated version of NJ-shape. With various research and experimental experience, the geometry of NJ-shape was optimized to get F-shape barrier, which has better performance with respect to crashworthiness requirements.

FHWA recommends the use of MASH guidelines for crash-testing procedures to evaluate the crashworthiness of concrete barriers (AASHTO, 2016). MASH, which was first implemented in 2009, is an update to NCHRP Report 350 (Millar & Authority, 1993), which was the standard for testing highway safety hardware before MASH. Beginning in 2016, FHWA requires any updates to NCHRP 350-tested devices to undergo the required testing under MASH. Both MASH and NCHRP 350 recommend the safety performance evaluation criteria as a function of three important factors: 1) structural adequacy, 2) occupant risk, and 3) post-impact vehicular response. Structural adequacy mainly focuses on barrier stability and ability to contain and redirect the vehicle (Michie, 1993).

Full scale, physical crash testing of PCB is recommended both by NCHRP 350 and MASH to test the safety provided by the barriers. As it is expensive to do real crash tests for each modification made to the safety features, FEM simulation is often utilized with results validated by physical testing. While MASH acknowledges the use of LS-DYNA in initial design procedures and its use by developers to assess the impact performance of safety features, it

requires actual crash tests to be conducted before barriers can be implemented for use (Michie, 1993; Millar & Authority, 1993).

The differences in the physical testing requirements between MASH and NCHRP 350 are compared in Table 2-1. A flowchart of the testing criterion is also presented in Figure 2.1.

Table 2-1 Comparison of Test Procedures for MASH vs. NCHRP 350

Test Level	**Test Vehicle**	**Vehicle Designation**		**Impact Conditions**	
		NCHRP	MASH	NCHRP	MASH
TL-3	Small Car	820C	1100C	1890 lb, 62 mph, 20° 820 kg, 100 km/h, 20°	2420 lb, 62 mph, 25° 1100 kg, 100 km/h, 25°
TL-3	Pickup Truck	2000P	2270P	4409 lb, 62 mph, 25° 2000 kg, 100 km/h, 25°	5000 lb, 62 mph, 25° 2270 kg, 100 km/h, 25°
TL-4	Single Unit Truck	8000S	10000S	17636 lb, 50 mph, 15° 8000 kg, 80 km/h, 15°	22000 lb, 56 mph, 15° 10000 kg, 90 km/h, 15°
TL-5	Tractor-Trailer	36000V	36000V	79366 lb, 50 mph, 15° 36000 kg, 80 km/h,15°	79300 lb, 50 mph, 15° 36000 kg, 80 km/h, 15°

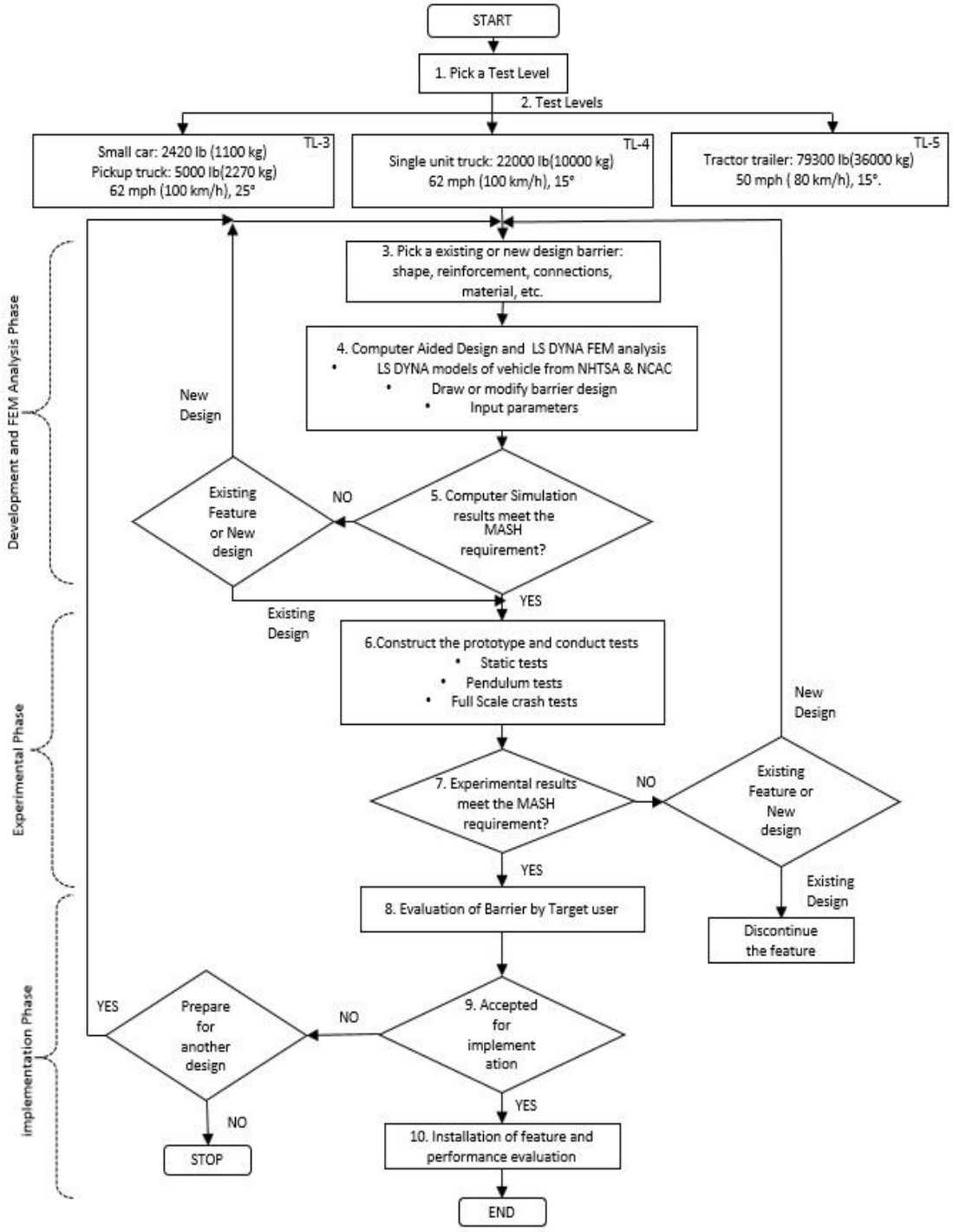

Figure 2.1 Flow Chart for the Development/Evaluation of a Safety Feature

Researchers in the past have used FEM techniques in conjunction with physical crash data to evaluate the safety performance of existing concrete barriers and have made recommendations to improve the existing designs. The general practice is to validate computer-generated models with a real crash test and to incorporate the new designs in the safety hardware.

2.2 Use of LS-DYNA to Test the Crashworthiness of Barriers

Albin et al. (2002) performed NCHRP test 3-11 on a baseline NJ-shape Washington state barrier with two sets of wire loop and a pin and validated the results with LS-DYNA simulation. FEM techniques were implemented to study various new types of connections. A full crash test for the selected improved connection design from LS-DYNA simulation, with three sets of steel bars as a loop instead of two sets of wire loop and a pin, was done and observed that the selected improved connection design had less deflection in the horizontal direction for the barrier and was considered safer (Albin, Bullard, Abu-odeh, & Menges, 2002)

Consolazio et al. (2003) conducted full-scale tests and LS-DYNA simulations on an 18-in tall (457 mm) by 12-ft (3.6- m) long low-profile barrier that was truncated at the striking side. The barrier was able to contain and redirect a 2000P vehicle as per NCHRP TL-2 and TL-3 requirements. As a result of this experiment, new connection designs were proposed for low-profile barriers (Consolazio, Chung, & Gurley, 2003). Marzougui et al. (2004) modified the NJ-shape barrier with pin and loop joints with three different designs: cover plate model, tapered shims model and separator block model. In the cover plate model, the U-channel plate in the concrete was bolted at four locations to connect the barriers. In the tapered shims model, two tapered wedges were added at each joint and fitted between loop and pin. In the separator block model, along with the loop-and-pin design, a 0.24 in (6 mm) thick separator block with four holes was fitted. To test the safety of the proposed joints, a full-scale crash test on a NJ-shape barrier was performed in the field and compared with the equivalent LS-DYNA model. The PCB displacement and the vehicle Center of Gravity (CG) accelerations were compared and validated. On the basis model verification, FEM simulations for the NJ-shape baseline model and with joint modifications were performed. The FEM resulted in less displacement than the baseline model (Dhafer Marzougui & Eskandarian, 2004).

A 34-in (863 mm) high 12-ft (3.6 m) long F-shape barrier was used by Yontel et al. (2005) to perform the NCHRP report 350 TL-3 test. The PennDOT design F-shape barriers have joints that do not resist tension between the adjacent segments, but rather have a steel plate to connect the concrete segments. The ends of the barriers were anchored to prevent vertical and lateral movement of the ends during the impact. Different concrete models were used to compare the lateral displacement with the crash test, to suggest the best concrete model that can be used in LS-DYNA (Yonten, Manzari, Marzouqui, & Eskandarian, 2005). Atahan et al. (2006) performed a full-scale NCHRP Report 350 TL-3 test and FEM analysis on a baseline New York Portable barrier with I-shape connector and observed it to fail. The speed and time for the vehicle for redirection from the barrier, state of the vehicle being parallel to the barrier and exit from the barrier is compared to validate the model. FEM simulation with increased fillet weld between the flange and web of the I-shaped connector was done to observe improved performance. A full-scale test of the FEM was done, which resulted in exit of the vehicle from the crash in a stable manner and lateral deflection to fall within approved limits (Atahan, 2006).

Itoh et al. (2007) performed a full-scale test and simulation with a 44000 lb (20000 kg) truck and a 164-ft (50 m) long and 55-in (1400 mm) tall CIP F-shape barrier with 11 in (300 mm) of the barrier buried under the road surface. This tall F-shape barrier had the ability to direct the movement of a truck to prevent it from leaving the road. The simulation and physical crash test were compared in terms of the displacement time histories of the barriers and were found to be similar (Itoh, Liu, & Kusama, 2007b, 2007a). The time-history displacement of the temporary barriers from simulation was compared to the real crash test as shown in Figure 2.2, and they were found comparable.

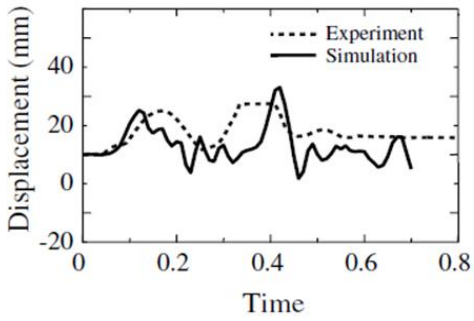

Figure 2.2 Time History Comparison of Real Crash Test and FEM (Itoh 2007)

Marzougui et al. (2007) performed an evaluation of five different shapes of barrier (F, NJ, Single Slope, Vertical, Inverted) with four different lengths: 6 ft, 10 ft, 12 ft and 20 ft (1.8 m, 3 m, 3.6 m and 6 m, respectively), two different barrier widths (narrow and wide), two different barrier gaps (open and closed) and two difference hook distances (close and far). Physical crash testing under NCHRP 350 TL-3 was performed with a 2000P vehicle and the F-shape PCB. The vehicle was a 4497-lb (2040.8 kg) Chevy C2500 pickup truck with recorded impact speed of 63.9 mph (102.9 km/h) and 23.8° impact angle. The acceleration readings from the CG of the vehicle and high-speed video images were recorded as the output parameters. The FEM for equivalent test was simulated using LS-DYNA and was validated by comparison of four responses: 1) Ride down acceleration, 2) Ride down velocity, 3) Rotation angle and 4) Barrier displacement. 160 different FEM combinations for the aforementioned different shapes, lengths, width, barrier gaps and hook distances were created and simulations were run to determine the crashworthiness of new designs. The FEM results were tabulated for each of the combinations.

This research concluded that longer barriers had better displacement response than shorter ones. NJ-shape barriers showed more tendency for the vehicles to roll over whereas Vertical, Single Slope and Inverted shapes had better performance in terms of the rotation angles. However, Vertical, Single Slope, and Inverted shapes increased ride down accelerations (Dhafer Marzougui, Buyuk, & Kan, 2007).

Esfahani et al. (2008) investigated the 32-in, 37-in and 42-in (810 mm, 940 mm and 1067 mm) NJ-shape and F-shape barrier as per the updated NCHRP test requirement TL 4-12, with a 22000-lb (10000 kg) single unit truck (SUT) at the speed of 56 mph (90 km/h). Using both physical crash test and LS-DYNA simulation, it was observed that the 32-in (812 mm) F-shape and NJ-shape barriers were not able to contain and redirect the vehicle. The roll and yaw angles and longitudinal velocity time histories of both the real crash test and simulation matched.

FEM simulation for 37-in (940 mm) and 42-in (1067 mm) barriers with the same input conditions resulted in containment and redirection of the vehicle. However, 37-in (940 mm) barriers were just enough to keep the maximum roll of vehicle below 40° and took longer time to reach zero roll. In the case of 42-in (1067 mm) barriers, the vehicle rolled up to a smaller angle and stopped rolling sooner (Esfahani & Opiela, 2008). One of the evaluation techniques used to

compare the FEM simulation with the real crash scenario is shown in Figure 2.3. This figure is taken from the research paper by Esfahani et al. and shows a comparison of the displacement history of temporary barriers in simulation.

Figure 2.3 FEM vs Real Crash Test of an SUT (Esfahani, 2008)

Atahan et al. (2009) used LS-DYNA simulation to test NJ-shaped barrier with four different heights: 32 in, 37 in, 40 in and 42 in (810 mm, 950 mm, 1000 mm and 1067 mm) with two different types of Heavy Goods Vehicle (HGV) as per EN 1317 standards (TB42: 70 km/h, 15°, 10000 kg and TB71: 65 km/h, 20°, 30000 kg) and studied the post-impact stability of the vehicle. The TB42 vehicle was contained by 32-in (810 mm) high barrier whereas a TB71 vehicle required a 42-in (1067 mm) barrier to contain it (Atahan, 2009).

In 2011, the National Academy of Sciences published a book of guidelines for the steps necessary to follow for verification between the computational modeling, carried out using LS-DYNA, and physical testing. The book illustrates how simulated and physical test data can be compared and provides the information on acceptance criteria. The Sprague-Geers Magnitude-

Phase-Comprehensive (MPC) and Analysis of Variance (ANOVA) metrics are described as preferable statistical methods to decide whether simulation results are acceptable in comparison with the physical tests. The material models, vehicle models and roadside safety hardware models used in LS-DYNA by different researchers are reviewed in a different section in this book. Four cases of vehicle crashes are illustrated and guidelines are given for how the verification and validation can be done by using Roadside Safety Verification and Validation Program (RSVVP) software ("Procedures for Verification and Validation of Computer Simulations Used for Roadside Safety Applications," 2011).

Marzougui et al. (2012) tested 32-in (810 mm) NJ-shape barriers to study whether the barrier that was considered safe under NCHRP Report 350 was also considered safe under MASH TL-3 with a 2270P test vehicle. The results suggested that the NJ-shape barriers that passed the evaluation of NCHRP 350 also performed well under MASH evaluation. Full-scale crash testing was compared with the LS-DYNA simulation and it was found to be comparable. The results from the test and simulation were then verified and validated using RSVVP software, which is recommended by NCHRP Project 33-24 (Dhafer Marzougui, Kan, & Opiela, 2012).

Sheikh et al. (2014) performed a full-scale MASH TL-3 crash test with a 2270P vehicle and 32-in (810 mm) tall, 12.5-ft (3.81 m) long F-shape barriers that were pinned down from the traffic side at a 45° angle to the bridge deck or pavement. The barriers were joined with a pin-and-loop-type connection to form a 100-ft (30.48 m) installation. The maximum permanent and dynamic deflections of the barrier were 5.76 in (0.146 m) and 11.52 in (0.293 m). The truck was successfully contained and redirected. FEMs from LS-DYNA were used to predict the design for the barriers (Sheikh, Bligh, & Fossier, 2014).

Abraham et al. (2016) used F-shaped barrier to demonstrate that higher impact angles have higher Acceleration Severity Index and higher Impact Severity, validating their simulation and real crash test results through RSVVP software. They concluded that the MASH standards that require car and pickup truck impact angles to be 25° are better than European standard EN 1317, which requires 20° (Abraham, Ghosh, Simms, Thomson, & Amato, 2016).

Yin et al. (2016) compared their FEM based on MASH TL-3 conditions with the real crash test performed by Marzougui et al. (2014) to validate their model and further applied

metamodeling techniques using Radial Basis Functions (RBFs) to optimize the cross section of NJ-shape concrete barrier. The height and bottom width of the barrier were kept constant. The top and bottom face of the barrier which comes in contact with the vehicle during impact plays an important role in the redirection of the vehicle. Thus, the cross-sectional dimensions at the top and bottom were the parameters optimized in the barrier shape. LS-DYNA was used to evaluate the objective and constraint values of initial samples generated by statistical procedures. Maximum absolute roll angle (MARA), which relates to vehicle rollover after impact, is very sensitive to the shape of the barrier. Thus, it is selected as the parameter to study the safety performance. The MARA values for different cross sections were evaluated and optimal design was suggested. The MARA of the colliding vehicle reduced for the optimized design as compared to the original NJ-shape and other safety criteria were also within MASH limits. Though the optimal design resulted in greater vehicle stability, it was observed that except for the MARA, other safety criteria like occupant impact velocity, occupant ride down acceleration and exit angle did not change significantly (D Marzougui, Kan, & Opiela, 2014; Yin, Fang, Wang, & Wen, 2016).

Schrum et al. (2016) used LS-DYNA to calculate strain energy in barrier and change of internal energy in the vehicle and compared those values with the Yield Line Method (YLM) to investigate the design of different shapes and barrier heights as proposed by MASH TL-4 and TL-5. In the research it was observed that tall barriers experience less load (including the barrier deck interface) but create a longer moment arm with higher resulting moment loads, which make it more susceptible to failure. It was concluded that since taller barriers are more susceptible to impact with cargo beds that contribute to overall damage, taller barriers have less capacity unless they are given more reinforcement. The researchers disagree with the recommendation from other researchers to increase the transverse load design in TL-4 and TL-5 barrier models. Their reasoning behind this is that, although the simulation from LS-DYNA shows that the cargo bed of vehicles comes in contact with the barrier, the research team did not observe contact between 36-in (915 mm) barrier and the cargo bed in physical tests. Being based on a modified YLM method, the AASTHO recommendation for the transverse design loads was determined to be appropriate (Kevin Schrum, Dean Sicking, 2016).

Kim et al. (2018) performed a full-scale crash test on 50-in (1270 mm) tall permanent improved Korean F-shape barrier. The data compared with the simulation results for validation and verification were vehicle exit speed, exit angle, vehicle rolling, damaged length, damaged height and fragmentation of central median barrier. Improvement techniques for 50-in (1270 mm) tall improved Korean F-shape permanent concrete median barrier that are subjected to higher impact energy situations were suggested from the simulation done on the improved barriers. The performance of the median barriers developed based on simulation results was significantly better than the barriers that were in practice on Korean highways (Kim et al., 2018).

Wang et al. (2018) performed reliability analysis to test the probability of exceedance of MASH TL-3 limits of vehicle crash responses, particularly Occupant Impact Velocity (OIV) and Occupant Ride Down Acceleration (ORA) for NJ-shape barrier and 2270P truck. FEMs validated by other researchers were used for LS-DYNA simulation. Five different impact angles and vehicle weights were used to perform simulation and obtain responses for these inputs. Probabilities of failure for those responses are calculated using Monte Carlo simulation for these results. It was found that the probability that the current NJ-shape design exceeds the MASH limits of OIV and ORA is very small (Q. Wang, Fang, & Yin, 2018) .

2.3 Modeling Techniques for Vehicle and Barrier Impacts

Roadside safety hardware is constantly evolving with the need for higher passenger safety and changing crashworthiness requirements. It is costly and time consuming to test whether the existing or newly modified hardware will meet crashworthiness requirements. FEM software packages, such as LS-DYNA, can be used to determine the crashworthiness of this hardware. Although LS-DYNA is popular and considered reliable for simulation purposes, researchers generally validate and verify their model with the real crash test results before further using their model to test or develop new systems. Various steps are involved in the process of simulating vehicle crashes with concrete barrier. Vehicle and barrier geometries are drawn exactly in the same scale as the original drawing and simulation parameters like material models, contact between surfaces, velocities, friction, desired output stations and quantities, and others that are defined.

One technique that researchers have used to model the barriers is to use rigid 8-node solid hexahedral elements. As the barriers are not expected to fail except for minor aesthetic damage, they can be modeled as rigid elements with no failure. In this method, only the portion of the barrier in contact with the road surface and with another barrier is assumed to be elastic, where damage is expected. The solid elements are covered by shell elements because of their better contact behavior. Rebar and other structural details inside the PCB are not modeled in this technique. The pin-and-loop connections are modeled as the beam elements and covered with the shell elements for better contact. The pin-and-loop connections can be entirely modeled as shell elements, too. The pin-and-loop joints or other types of connections can be modeled as isotropic elastic material model available in the LS-DYNA material library (Atahan, 2006; Dhafer Marzougui & Eskandarian, 2004; Dhafer Marzougui et al., 2007). Barriers can also be modeled as only rigid shell elements assuming that deflection and deformation does not occur (Dhafer Marzougui et al., 2012).

Various material models for concrete are available in LS-DYNA. From various experiments and simulations researchers have found out that the Material Model 16 and Material 72 have better performance for simulating vehicle crashes into the barrier (Yonten et al., 2005). Material 16 or Material 72 are mostly used to analyze the buried reinforced concrete structures subjected to impulsive loadings (LSTC, 2012). Another way of modeling the concrete barrier is to include the reinforcement as well by defining the reinforcing bars as beam elements and use Hughes-Liu beam elements formulations ("F800 SUT Model," 2005; Itoh et al., 2007b, 2007a).

Modeling of the vehicle for crash simulation is a lengthy process. The vehicle model is available on the websites of NHTSA and other institutions, and can be downloaded to use for modification purposes as per the requirements (Borovinšek, Vesenjak, Ulbin, & Ren, 2007; "Crash Simulation Vehicle Models | NHTSA"). The vehicle body is mostly modeled as solid beam and shell elements. In the case of tires, researchers have modeled them as the airbag model with internal pressure ("F800 SUT Model," 2005; KA et al., 2006).

Defining an appropriate contact algorithm is very vital to get the desired results. Crash simulation with automatic surface-to-surface contact is most commonly used. This gives results without nodal penetration. Friction is another important aspect of modeling because it predicts

the interaction between the impacting vehicle and barrier. It also plays a role to determine the deflection of the barrier and rollover of the vehicle. Friction should be defined between any surfaces that are in contact with each other, such as: road surface and tires, tires and barrier, and vehicle body and barrier. Past studies have used both constant- and velocity-based μ values for the friction between the surfaces in contact. In some studies, the values of 0.45 and 0.40 are used as static and dynamic friction between the barrier and road surface and 0.35 to represent the frictional forces developed between the vehicle's parts and concrete barrier. In the case of the contact between the tires and the barriers, significant scrubbing contact occurs, thus it is better to choose a velocity-dependent friction model rather than a constant one (Atahan, 2006; Bligh, Sheikh, Alberson, & Abu-Odeh, 2006; Consolazio et al., 2003; KA et al., 2006; D Marzougui et al., 2014; Dhafer Marzougui et al., 2012; Trajkovski, Ambrož, & Kunc, 2018).

Monitoring the simulation to determine if the results are valid is another important step in vehicle crash simulation. To minimize the simulation time, integration points within an element can be reduced so that the stiffness matrices are calculated at fewer points. For example, for a fully integrated quadratic element, which has two integration points in each direction, LS-DYNA allows for a single integration point in each direction, which results in faster simulation time because fewer stiffness matrices are calculated to get desired results. This procedure can cause deformations that do not produce any stresses and strains. Such deformation processes, which do not contribute in FEM calculation and ultimately lead to bad results, are called hourglassing. If significant hourglassing is observed, the simulation results are considered unreliable. Hourglassing can be eliminated by using fully integrated elements but this can cause an increase in simulation time. LS-DYNA has an hourglassing control algorithm that can be activated for elements in under-integrated portions of the mesh. Thus, the ideal method would be to use fully integrated elements in contact zones and the areas where severe deformation is expected and to use under-integrated elements with the hourglass control algorithm in other areas (Consolazio et al., 2003; "Hourglass — Welcome to the LS-DYNA support site," 2020). Figure 2.4 illustrates the energy balance equation for a crash simulation in LS-DYNA. In the curve we can see the total energy being stable throughout the simulation whereas the decrease in kinetic energy and increase in sliding and internal energy add up to maintain the balance for total energy.

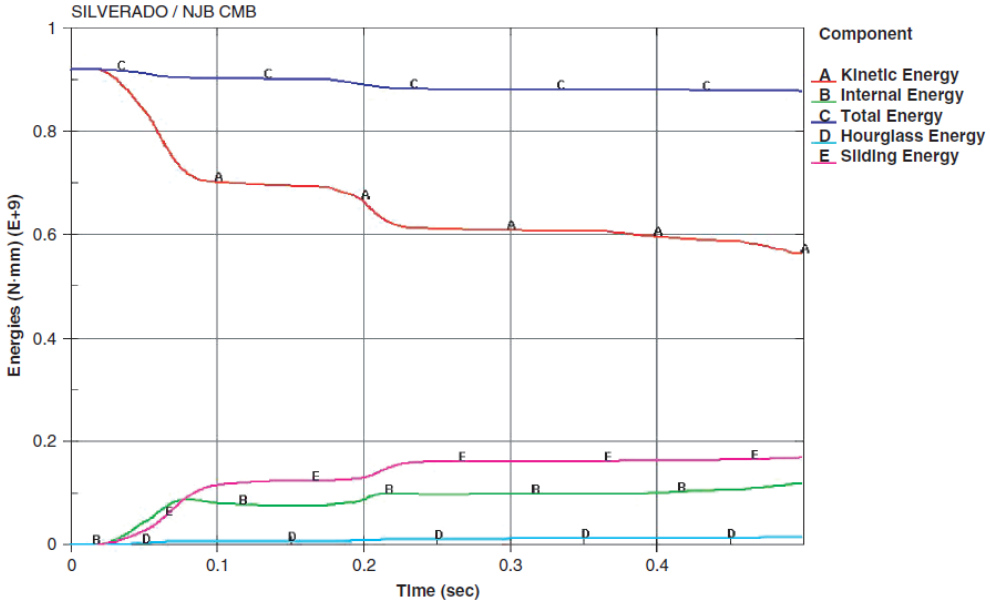

Figure 2.4 Energy Balance in Simulation (Esfahani, 2008)

2.4 Comparison and Validation of FEM Results

As per MASH, the safety performance of a highway safety structure is evaluated based on three parameters: Structural Adequacy, Occupant Risk and Vehicle Trajectory. Various values like deflection of the test articles, ability of the test article to control and redirect the vehicles, roll and pitching vehicles, exit angle, and exit speed are studied under these parameters.

One of the most significant parameters that is widely used to validate the FEM results with the crash test is the lateral deflection of the barrier and its ability to contain and redirect the vehicle. Researchers in the past have compared the deflection history of the barrier at different points after the impact for both the simulation and real crash test and considered their model validated if the deflection time history curve is similar. In addition to this approach, slow motion videos of real crash simulation are also compared with the output video of the simulation, and similarities in the motion and trajectory are studied. Another approach relates to kinematics. LS-DYNA offers abilities to model accelerometers to measure the deflection, acceleration and velocities of any rigid body and vehicle nodes in both local and global coordinates. These measurements can then be compared with the accelerometers that are placed in a similar location

in real crash tests. **Error! Reference source not found.** is a flowchart that explains the MASH evaluation procedure for a barrier.

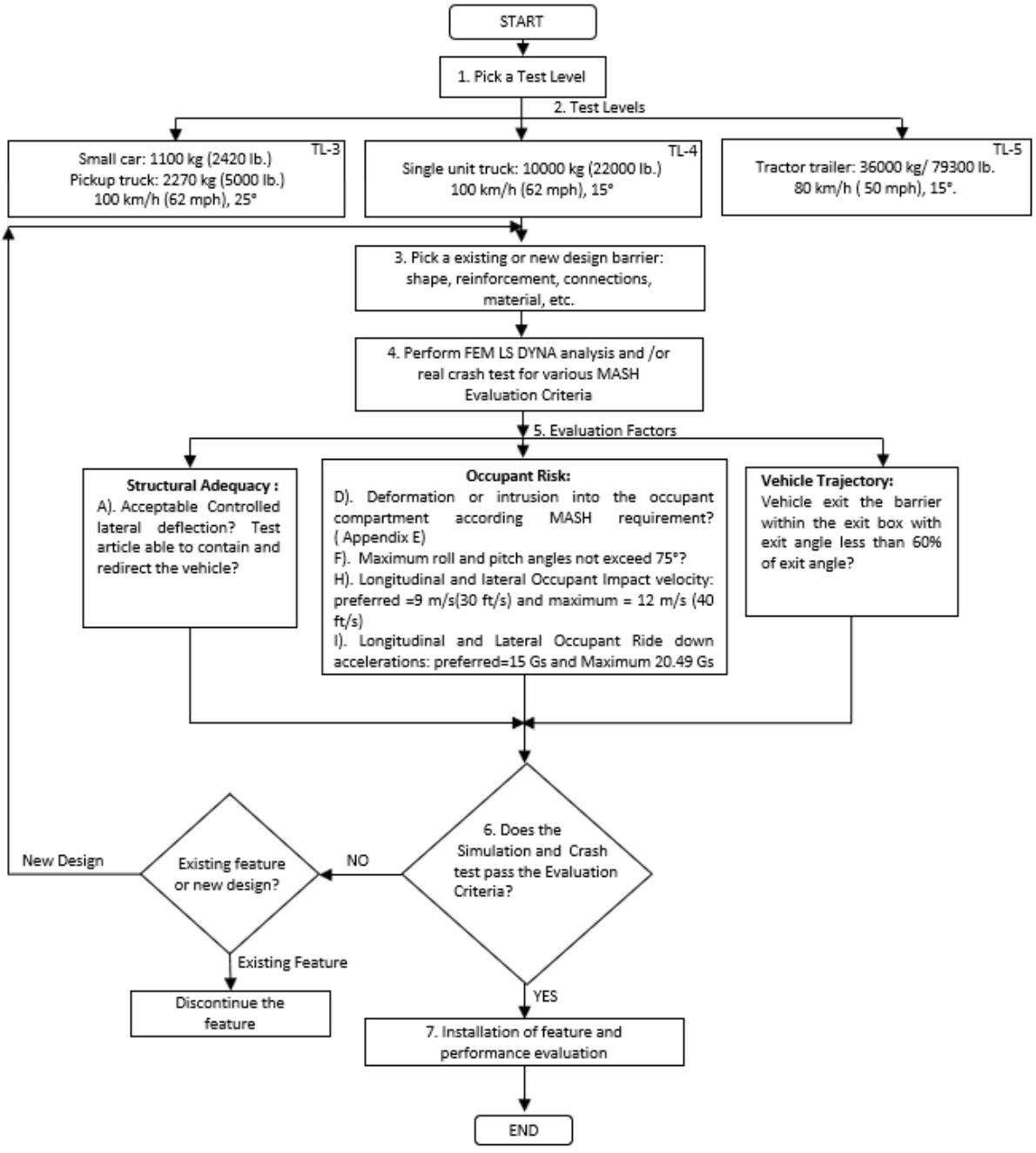

Figure 2.5 MASH Evaluation Procedure for a Barrier

Of the data acquired from accelerometers, time histories of roll and pitch, as well as accelerations in different directions of the vehicle can be analyzed. These accelerometer data are used to calculate occupant risk values like Impact Severity, Acceleration Severity Index, Theoretical Head Impact Velocity, and Post-Impact Head Deceleration which are important in determining the crashworthiness of a vehicle.

The NCHRP Project 22- 24 – "Guidelines for Verification and Validation of Crash Simulations Used in Roadside Safety Applications" has recommended a validation and verification procedure which involves use of the software package RSVVP. In this procedure, the change in acceleration in longitudinal, lateral and vertical direction along with roll and pitch for both the simulation and crash test rate are compared in a time history plot using the software. Statistical procedures like MPC and ANOVA metrics are implemented to compare the simulation versus crash test curves (Atahan, 2006; Bielenberg, B.W., Faller, R.K., Rohde, J.R., Reid, J.D., Sicking, D.L., and Holloway, 2007; Borovinšek et al., 2007; Dhafer Marzougui & Eskandarian, 2004; Itoh et al., 2007a; Lee, Shrivatri, & Ohara, 2017; Dhafer Marzougui et al., 2007; Yonten et al., 2005).

2.5 Conclusion

LS-DYNA is widely used by researchers for modeling simulation of vehicle crashes into barriers because of its ability to produce results comparable to real crash tests. Performing a real crash test every time to check the crashworthiness of barriers is an expensive process. LS-DYNA can be used to analyze existing as well as future new design barriers. Input parameters like impact speed, angle, shape of barrier, etc. can easily be changed and the output results can be compared, so that researchers and policy makers can get basic ideas about new designs that are to be implemented in the future. Since cargo loads are increasing, LS-DYNA can be an important tool to determine future updates to the barrier height and shape to be used in highways and bridge rails.

3. EVALUATION PROCEDURE

FEM models of the 42-in and 54-in (1067 mm and 1372 mm) barriers are developed in LS-DYNA. A baseline FEM for Midwest Guardrail System (MGS) barrier was provided by the Midwest Roadside Safety Facility (MWRSF) at the University of Nebraska-Lincoln. To evaluate the safety performance of these barriers, the FEM of MGS barrier was subjected to MASH TL-3 whereas the FEM of constant slope 42-in barrier was subjected to MASH TL-4 and the 54-in barrier was subjected to MASH TL-5 test conditions. In this research report, two evaluation factors, structural adequacy and occupant risk, are evaluated. In MASH, structural adequacy is defined in Group A, B and C of the evaluation criteria which are evaluated in this report. The occupant risk factors have various evaluation matrices divided into different groups D to H. In this report, the evaluation criteria from Group F is selected for analysis.

Table 3-1, gives a detailed explanation on how the evaluation factors of structural adequacy and occupant risk are analyzed as per MASH. The evaluation factors are subdivided into different groups which describe the evaluation criteria or process of analysis. Only the evaluation factors and criteria that are used in this report are presented in the table.

Table 3-1 MASH Safety Evaluation Guidelines

Scenario Number	Evaluation Factors	Evaluation Criteria
1	Structural Adequacy	A. Test article should contain and redirect the vehicle or bring the vehicle to a controlled stop; the vehicle should not penetrate, underride or override the installation although controlled lateral deflection of the test article is acceptable.
		B. The test article should readily activate in a predictable manner by breaking away, fracturing or yielding.
		C. Acceptable test article performance by redirection, controlled penetration or controlled stopping of the vehicle.
2	Occupant Risk	F. The vehicle should remain upright during and after collision. The maximum roll and pitch angles are not to exceed 75°.

4. TL-3 MASH EVALUATION OF MIDWEST GUARDRAIL SYSTEM (MGS)

4.1 FEM of MGS Barrier

The FEM has been verified with full-scale crash tests in the past and is ready to use in other simulation applications (Reid, 2009; Reid, Kuipers, Sicking, & Faller, 2009). The model has 180 different parts and 400,000 elements. The FEM replicates a 180-ft (55.5 m) long full-scale installation (Figure 4.1 & Figure 4.2). In this model the soil is modeled as rectangular hollow tubes with W6X9 steel posts inside them. The tubes are modeled by providing soil stiffness with the help of springs by defining its loading and unloading properties. The relationship between the steel post flanges and hollow tubes is defined by the *CONTACT _AUTOMATIC_SURFACE_TO_SURFACE command.

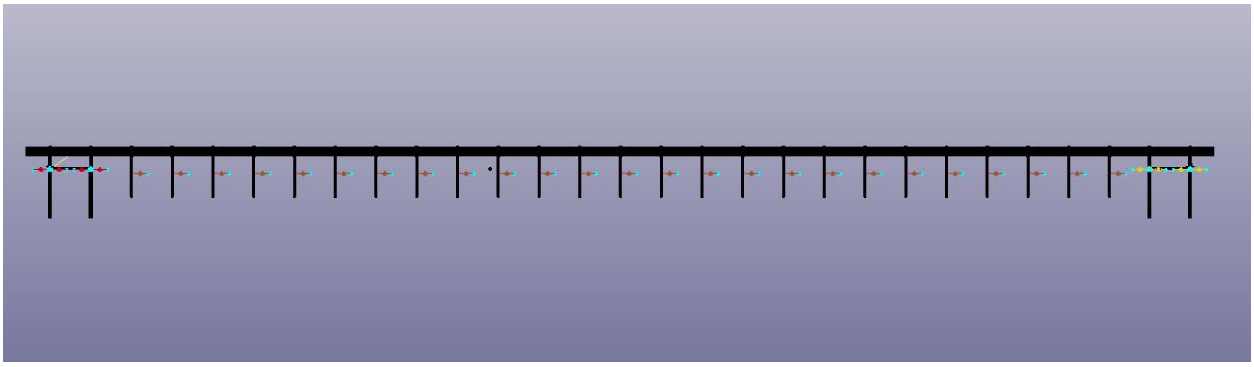

Figure 4.1 MGS Barrier Full-Scale FEM

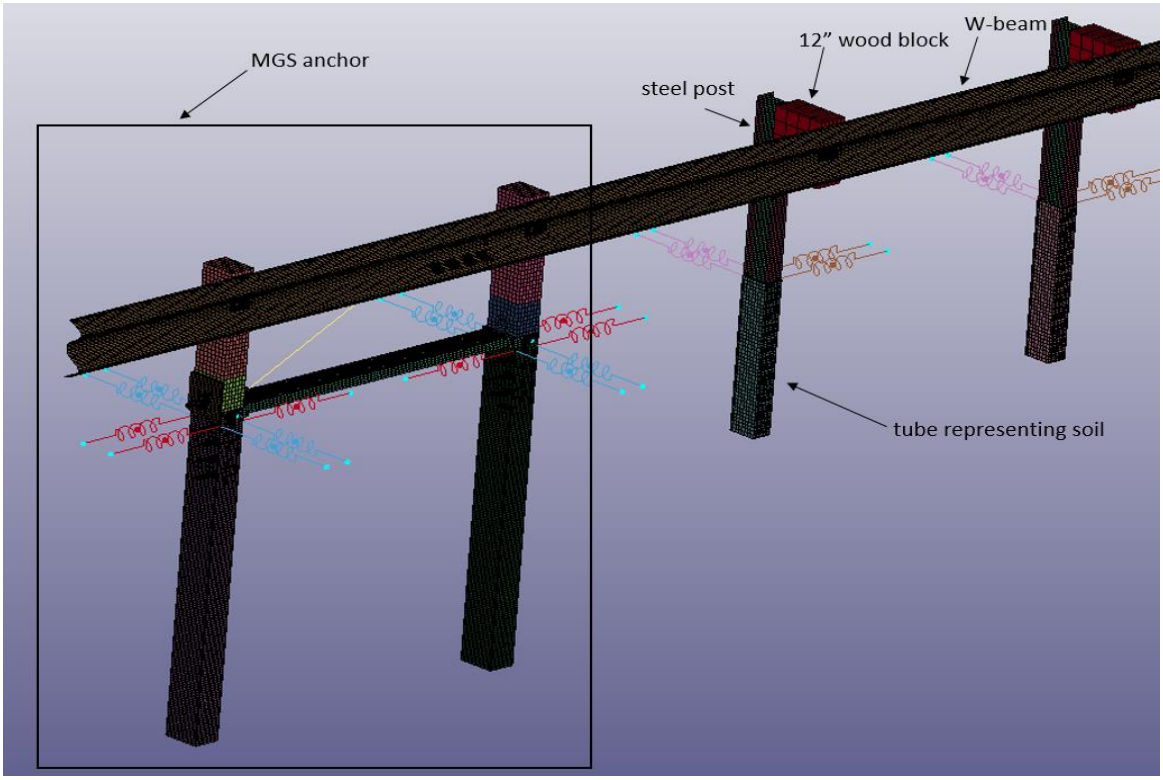

Figure 4.2 Different FEM Parts of MGS Barrier

4.2 FEM of 2007 Chevrolet Silverado Pickup Truck

The MASH TL-3 2270P was developed by the Center for Collision Safety and Analysis at George Mason University based on the 2007 Chevrolet Silverado pickup truck model. The model was validated against several full-scale crash tests. The mass of the truck is 5000 lb (2270 kg) as required by MASH TL-3. The FEM of the truck has 603 parts and 251400 elements. The vehicle velocity speed and direction are modified as per the requirement of this research.

Figure 4.3 represents the FEM of the 2007 Chevrolet Silverado pickup truck and Figure 4.4 represents the setup for the MASH TL-3 test where the vehicle is at a 25° impact angle.

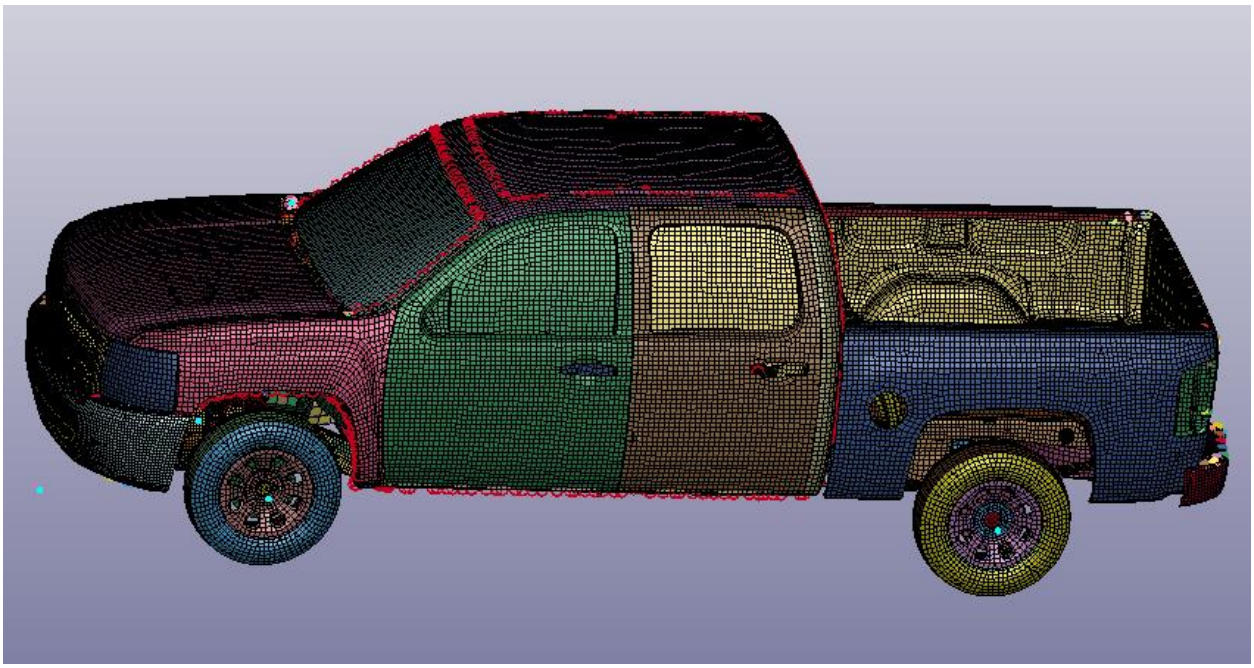

Figure 4.3 FEM of MASH TL-3 Pickup Truck

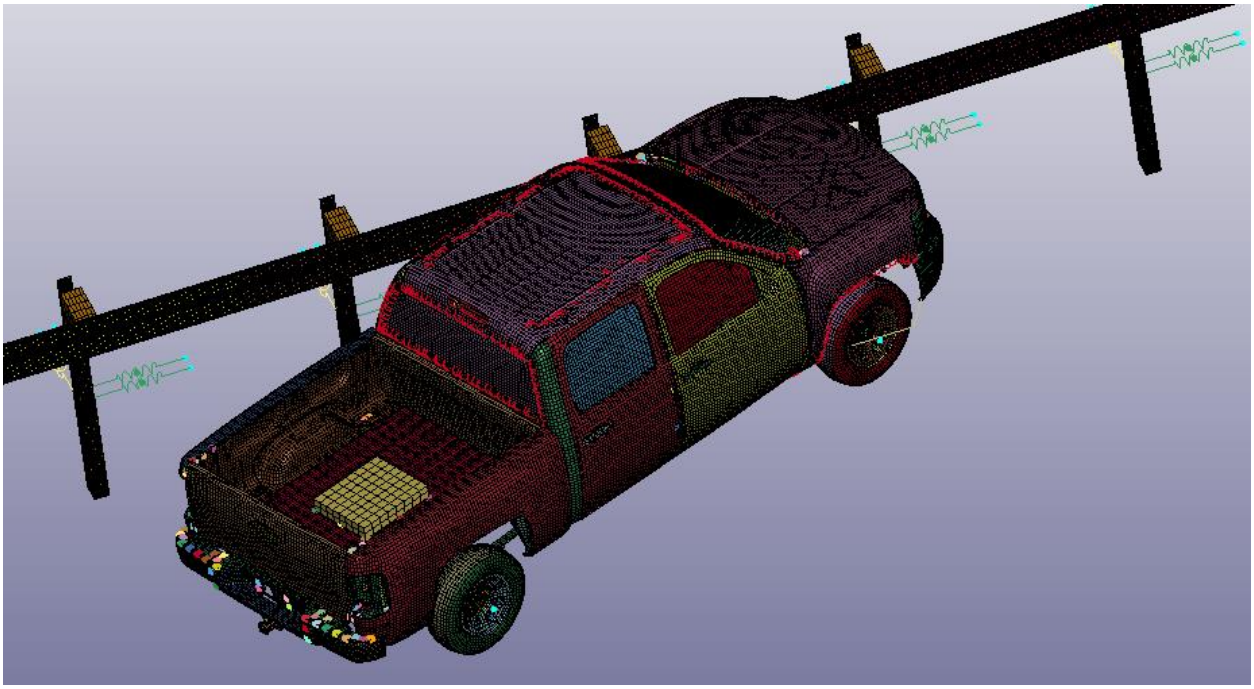

Figure 4.4 MASH TL-3 Setup for MGS Barrier

4.3 Validity of TL-3 MGS Model

The energy balance equation for the simulation of MGS barrier with a MASH TL-3 test vehicle is shown in Figure 4.5. The total energy is taken as constant, while the decrease in kinetic energy and summation of increase in internal energy and sliding energy are equivalent. The hourglass energy is determined to be negligible. Thus, the simulation can be considered valid since the total energy is conserved.

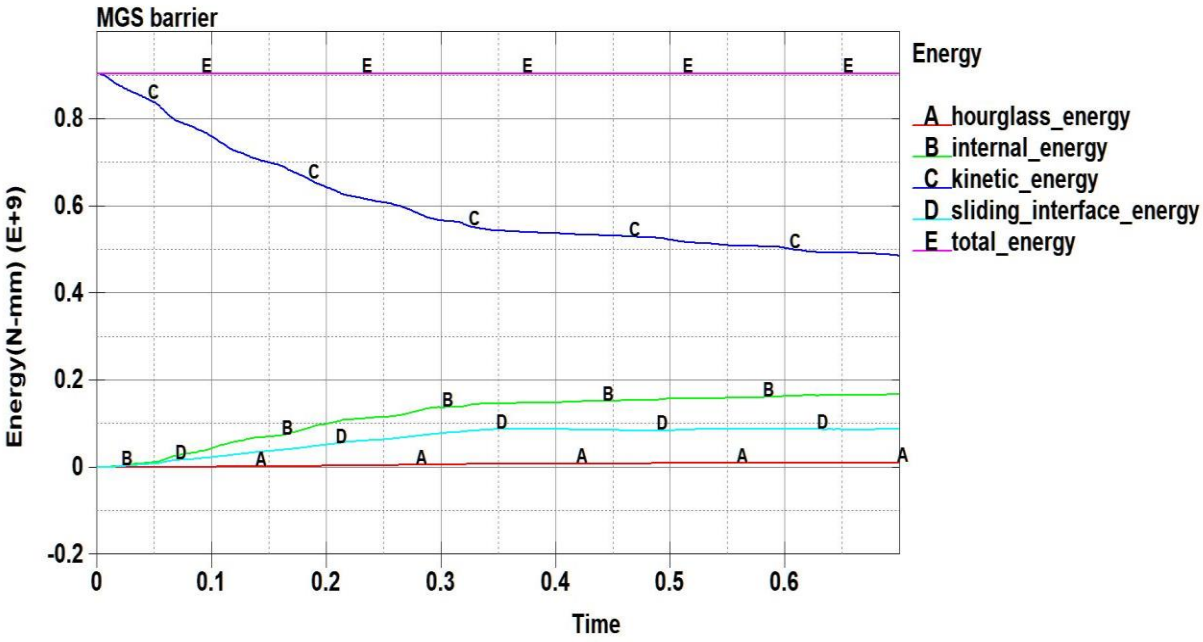

Figure 4.5 Energy Balance Equation for Simulation of MGS

4.4 TL-3 Crash Simulation Time History of MGS Barrier

The crash simulation is illustrated in the subsequent figures of this section. The figures show the different state of the truck during the crash simulation. Figure 4.6 shows the truck at the state just before the crash. Figure 4.7 shows the failure of first wooden block off the W-beam. In Figure 4.8 it can be observed that several wooden blocks fail off the W-beam whereas in Figure 4.9 it is observed that the steel post is crushed by the truck. In Figure 4.10 it is observed that the truck starts to divert from the barrier. Figure 4.11 shows that the front wheels of the truck divert away from the barrier. Finally, in Figure 4.12 it is observed that the truck is diverted away from the barrier with W-beam intact.

Figure 4.6 At t=0 s, Before Strike

Figure 4.7 At t=0.05 s, the First Wooden Block Fails

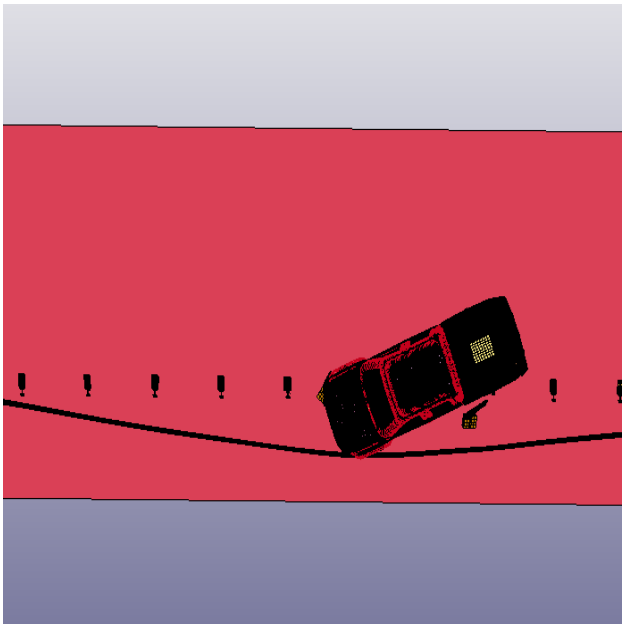

Figure 4.8 At t=0.205 s, Several Wooden Blocks Fail

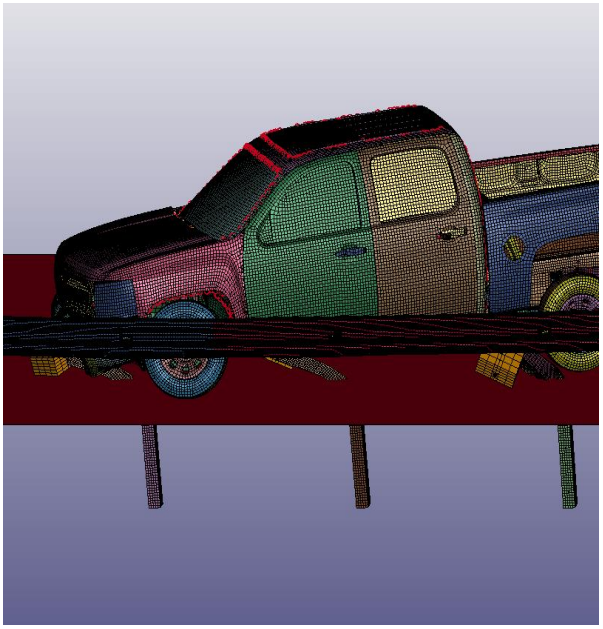

Figure 4.9 At t=0.205 s, the Steel Posts That Come in Contact with Truck Fail

Figure 4.10 At t=0.355 s, the Vehicle Starts to Divert Back into the Roadway

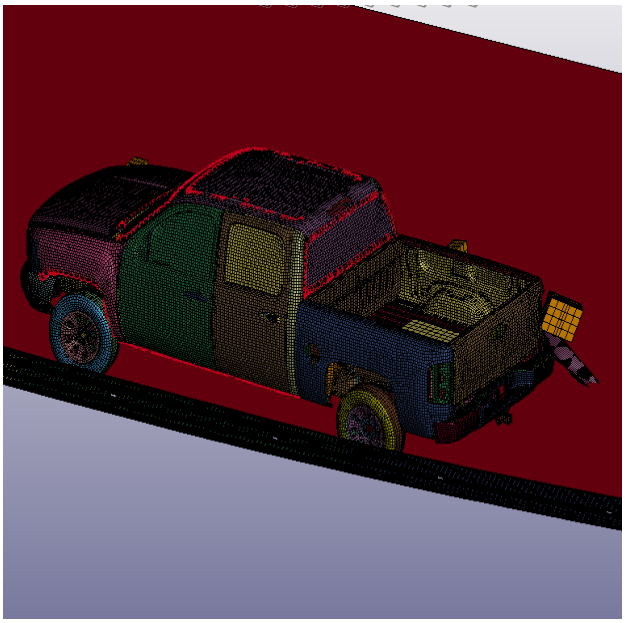

Figure 4.11 At t=0.535 s, the Front Wheel of Vehicle Moves Away from Barrier While Diverting Back

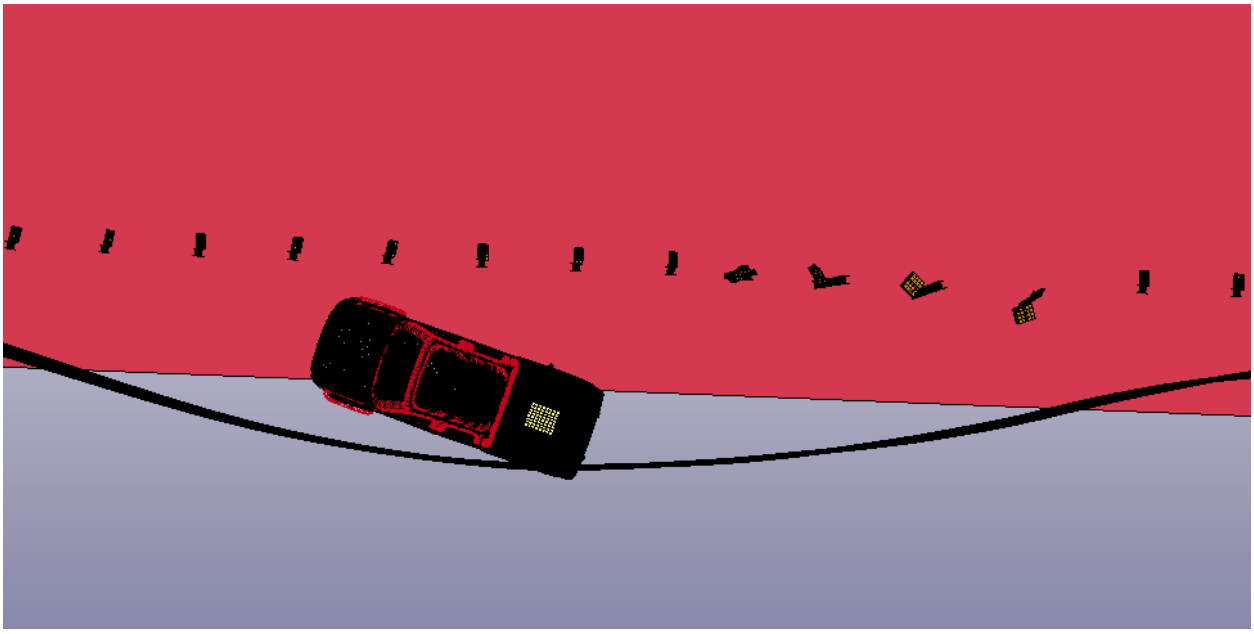

Figure 4.12 At t=0.7 s, the Vehicle is Diverted While the W-Beam Failed from the Posts

4.5 Structural Stability of MGS Barrier

After the full-scale crash simulation of the 180-ft (55.5 m) long MGS barrier, the pin-and-bolt connection between the wooden block and the W-beam failed in most of the posts (Figure 4.13). The posts that came in contact with the truck were crushed. It was observed that the W-beam rails that were spliced at the center between posts did not fail and acted as important factors to reduce the velocity of the vehicle towards controlled stop and to redirect the vehicle. Figure 4.14 shows the truck velocity reduction with time after crashing into the MGS barrier. The maximum displacement of the W-beam rail is about 13 ft (4 m) (Figure 4.15).

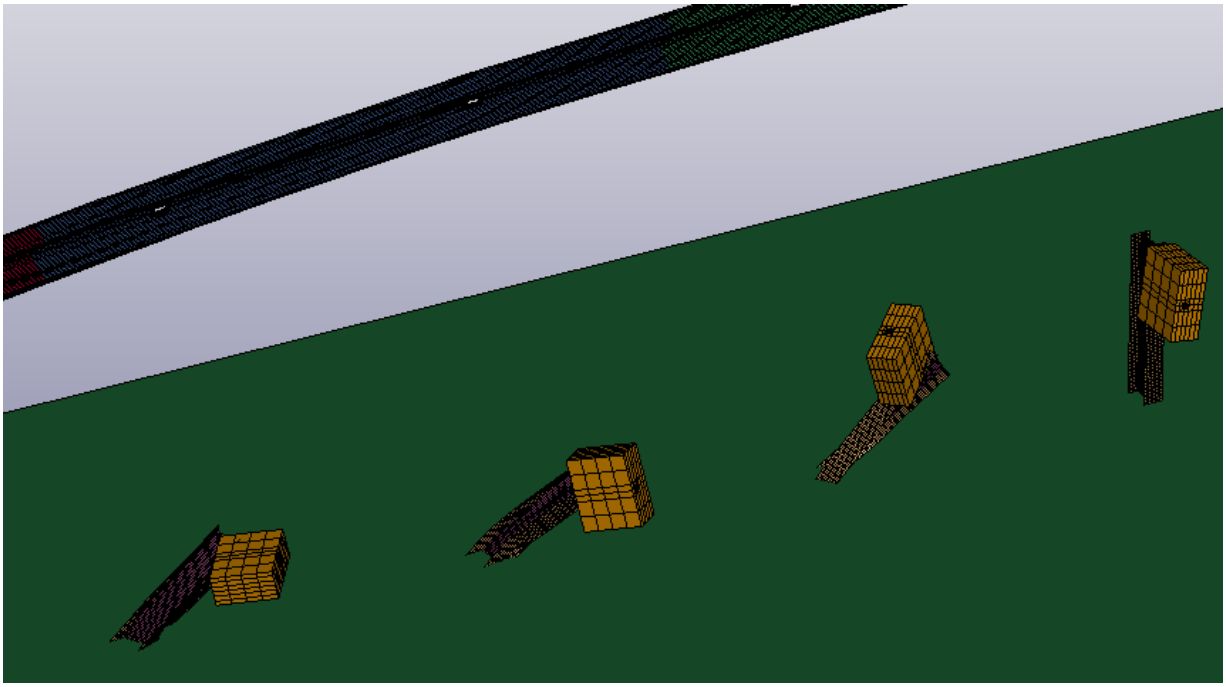

Figure 4.13 Failure Between The W-Beam, Wooden Block and Post

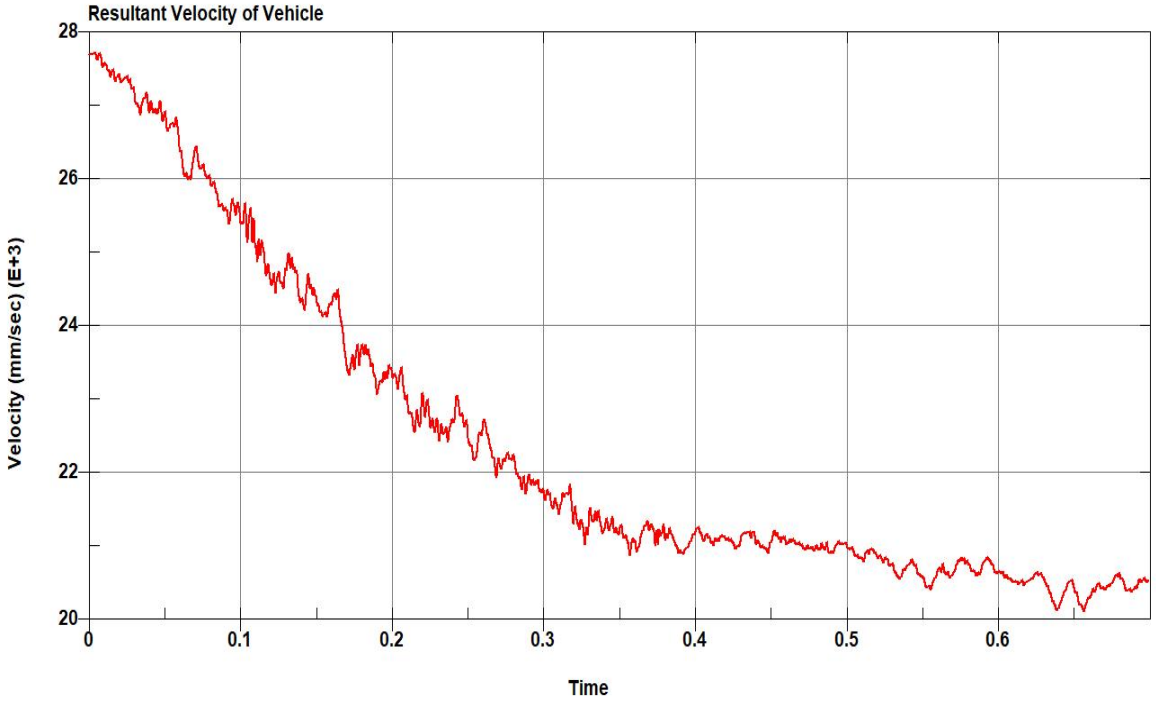

Figure 4.14 Resultant Velocity of the Truck after Impact with MGS Barrier

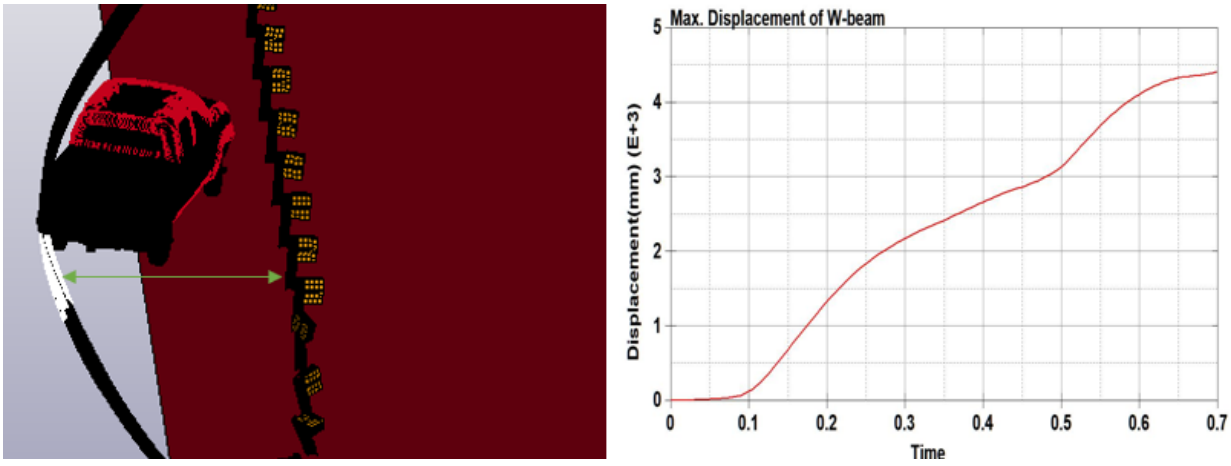

Figure 4.15 Maximum Displacement of W-Beam

4.6 Summary: MASH TL-3 Evaluation Criteria for MGS Barrier

Table 4-1 presents the evaluation criteria for MGS barrier subjected to MASH TL-3 evaluation criteria. The vehicle is observed to be diverted safely and it did not override or underride the installation. The barrier was damaged in the predicted manner. Since MGS is not a rigid barrier, large displacement of its components is expected. Thus, the barrier passes Criteria A, B and C of the MASH evaluation for structural adequacy.

Table 4-1 MAST TL-3 Evaluation for MGS Barrier

Factor	Criteria	Result	Comments
Structural Adequacy	A	Satisfactory - Pass	Vehicle did not penetrate or override the installation, although displacement of barrier was high
	B	Satisfactory - Pass	The test barrier activated in a predictable manner by fracturing
	C	Satisfactory - Pass	The test barrier redirected the vehicle and controlled stoppage of the vehicle was achieved

5. MASH TL-4 EVALUATION OF UDOT 42-INCH CONSTANT SLOPE BARRIER

5.1 FEM of 42-in Barrier

The safety performance of any longitudinal barrier is the function of its shape (i.e., slope and height). The FEM of the barrier is developed in two phases. In the first phase, instead of modeling the concrete and reinforcement, the barriers are modeled as solid shell elements to save computation time. A 3D model of the barrier is drawn in LS-PrePost. The solid shell is covered with the null shell elements to capture the behavior of contact. Each section of the barrier is 12 ft (3.66 m) long with a 10-in (254 mm) expansion joint provided at the end of each barrier. The element size of the null and rigid shells is 7.87 in (200 mm). The ground road is modeled as a rigid shell element and the barriers are fixed to the ground for displacement and rotation in all directions using the BOUNDARY_SPC element. Figure 5.1 represents the cross-sectional view and Figure 5.2 represents the isometric view of the 42-in (1067 mm) FEM barrier.

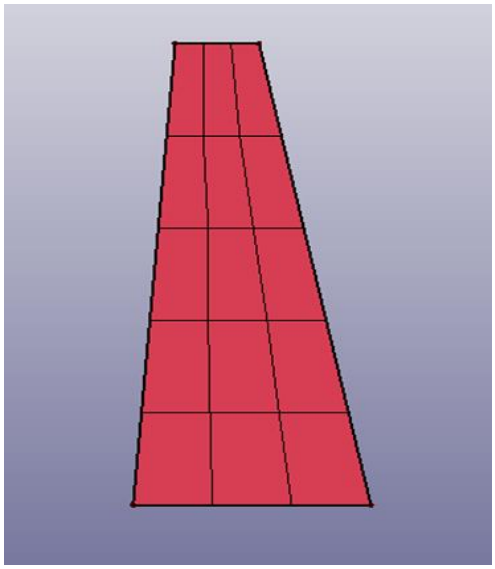

Figure 5.1 Cross-Section View of 42-in (1067 mm) Barrier

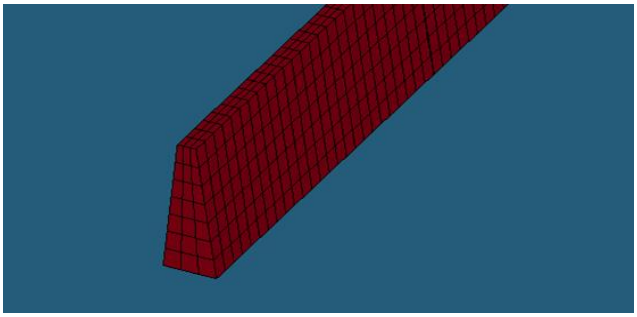

Figure 5.2 Isometric View of 42-in (1067 mm) Barrier

In the second phase, after the safety performance of the barrier is analyzed, the full-scale model of barrier is prepared as per UDOT specifications. A 40-ft (12192 mm) long barrier section is modeled on PCCP base. The PCCP base is 2-ft (0.61 m) wide and 10 in (250 mm) in depth, so that it is sufficient to incorporate the dowel bars into them and provide the base for

barrier. The model of barrier, base and ground is shown in Figure 5.3 and Figure 5.4 represents the FEM of dowel bars and base. Both the barrier and base are modeled in tetrahedral solid elements and MAT 159-CSCM_CONCRETE is used to model the material property of the concrete for both barrier and base. The strength of concrete is taken as 4350 psi (30 MPa). The concrete-to-hardened concrete surface was modeled by providing a static friction coefficient equal to 1 as per ACI 318-14. Reinforcing bars are modeled explicitly in such a way that the concrete and reinforcement do not share common nodes. Arbitrary Lagrangian-Euler (ALE) method with keyword *ALE_COUPLING_NODAL _CONSTRAINT is used to couple reinforcement and concrete where concrete is selected as the master part and reinforcement is selected as the slave part. Figure 5.5 represents the 42-in barrier reinforcement FEM. The longitudinal rebars, stirrups and dowel bars are modeled as beam elements with Hughes-Liu beam element formulations. The reinforcement is modeled as a MAT-PIECEWISE_LINEAR_PLASTICITY material with the stress-strain curve as shown in Figure 5.6.

The initial angle of impact between the test vehicle and the barrier is set at 15°. This is the angle specified by the MASH criterion. The test criterion is then evaluated according to the procedure developed in section 2.4 and the flowchart in Figure 2.5.

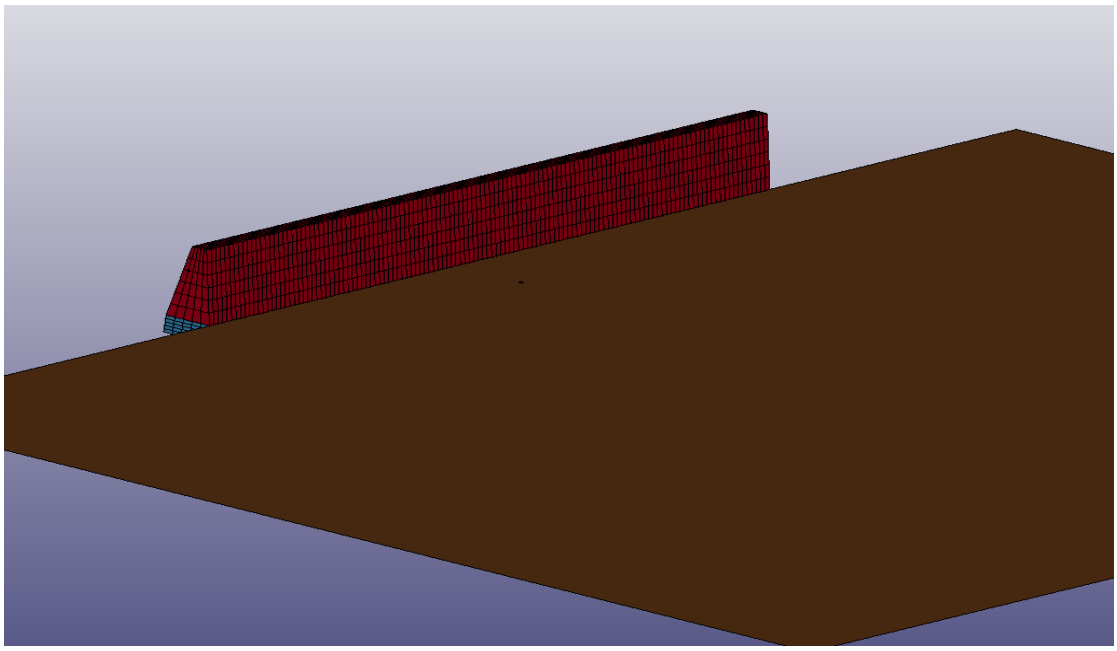

Figure 5.3 FEM of Barrier, Base and Ground

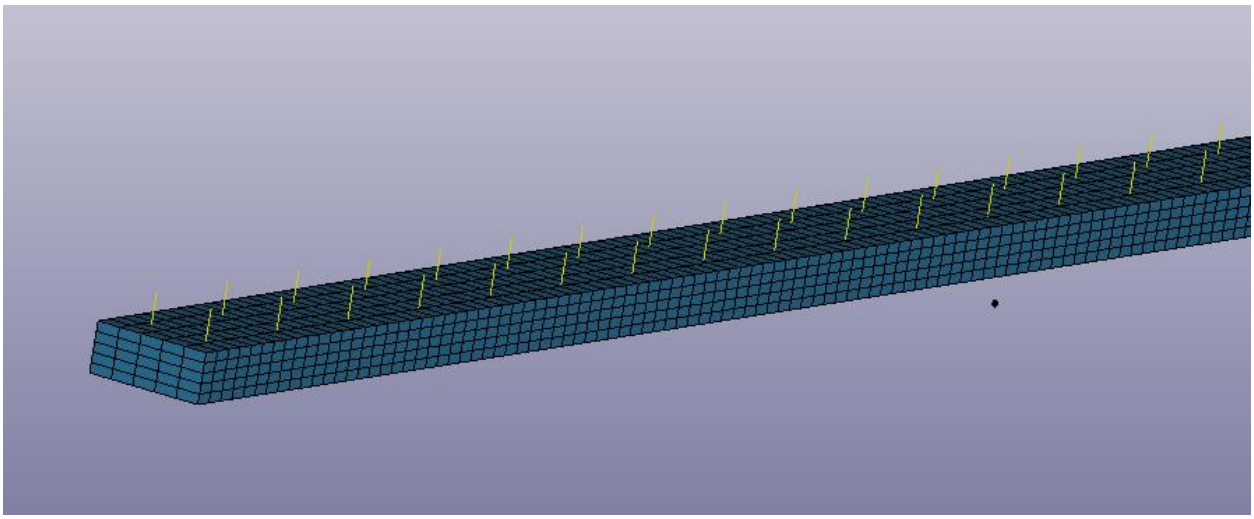

Figure 5.4 FEM of Dowel Bars and Base

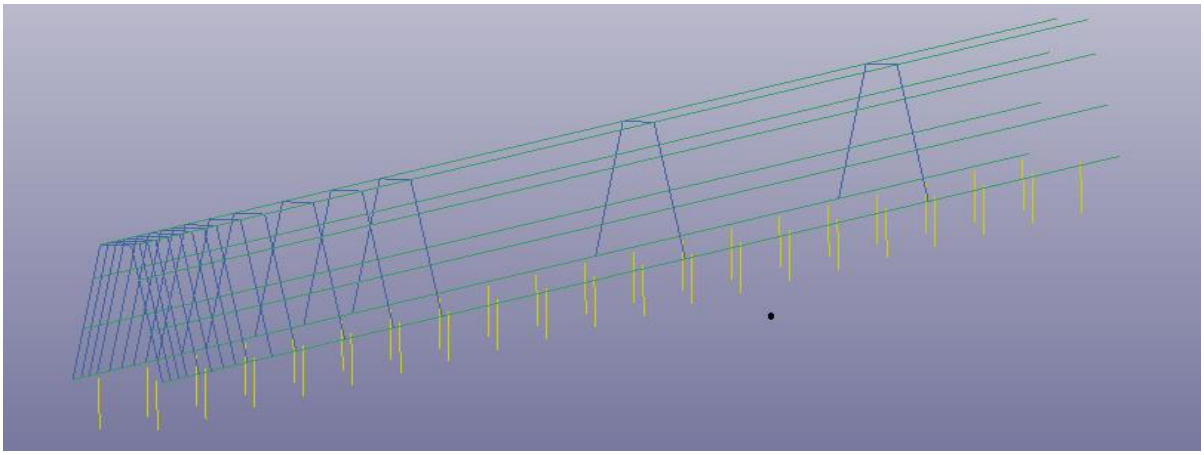

Figure 5.5 Barrier Reinforcement FEM

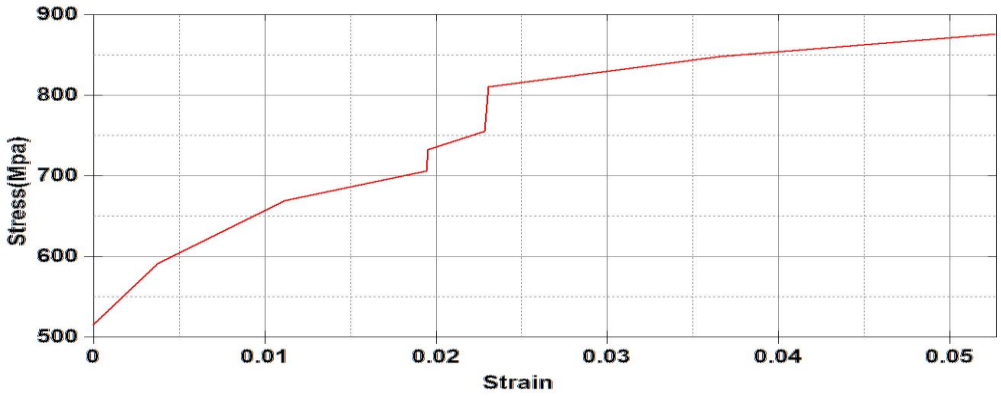

Figure 5.6 Stress-Strain Curve for Reinforcement Bars

5.2 Consistent Unit in LS DYNA

Although the inputs of length, mass and time are unitless in LS-DYNA, the units should be consistent (i.e., the same units should be followed throughout all the physical quantities). In this report for modeling and simulation of TL-4 and TL-5 barriers, the consistent unit of ton is used for mass, mm is used for length and s is used for time. Therefore, all the outputs are expected as the combination of these units. For example, velocity is in mm/s and energy is in N mm.

5.3 FEM of SUT

A Ford F800 SUT (TL-4) was originally developed by the National Crash Analysis Center (NCAC) at George Washington University (GWU). Improvements were made by Oak Ridge National Laboratory (ORNL) and the University of Tennessee at Knoxville. The weight of the SUT along with the cargo load is 10.05 Tons. The FEM of the truck has 154 parts and 35240 elements and is shown in Figure 5.7. Figure 5.8 shows the FEM of the SUT, barrier, and ground compiled together as input in LS-DYNA. The FEM of the SUT has been validated against the real TL-4 crash test on numerous occasions by previous researchers (“F800 SUT Model,” 2005; S. Wang et al., 2011).

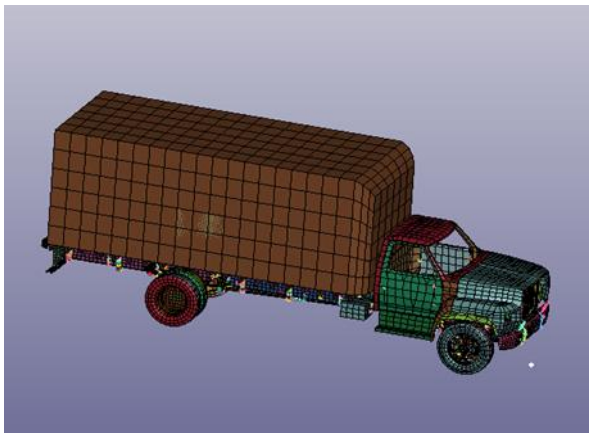

Figure 5.7 FEM F800 SUT

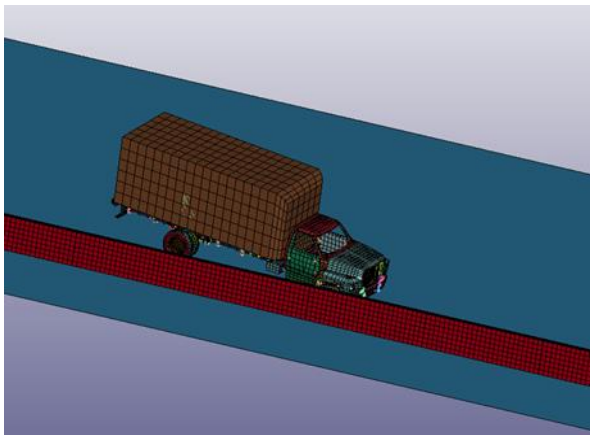

Figure 5.8 FEM Truck and TL-4 Barrier

5.4 Validity of TL-4 Model

The energy balance equation for the simulation of 42-in (1067 mm) barrier with a MASH TL-4 test vehicle is shown in Figure 5.9. The total energy is constant, while the decrease in kinetic energy and summation of increase in internal energy and sliding energy is equivalent. Hourglass energy is treated as negligible. Thus, the simulation can be considered valid because the energy is conserved.

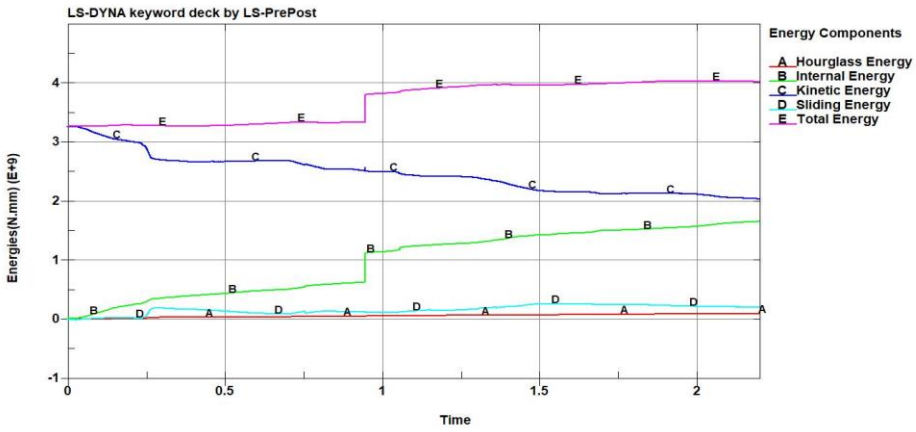

Figure 5.9 Energy Balance Equation for Simulation of TL-4 42-in (1067 mm) Barrier

5.5 TL-4 Crash Simulation Time History Description

The TL-4 SUT crash simulation in the 42-in (1067 mm) constant slope barrier is 2.2 s long. The vehicle is observed to divert safely away from the barrier after the impact, although severe damage is observed in the vehicle. The crash simulation is illustrated in the subsequent series of figures. **Error! Reference source not found.** shows the state of the SUT before impact. In **Error! Reference source not found.**, the SUT is observed to have frontal crush at t=0.09 s and the front part of the vehicle is observed to divert away from the barrier at t=0.16 s as observed in **Error! Reference source not found.**. In **Error! Reference source not found.** the trailer is observed to override the barrier at t=0.2 s. The back tires come in contact with the barrier at t=0.28 s as observed in **Error! Reference source not found.** and the back tires ride the barrier and slide against it at t=0.32 s as observed in **Error! Reference source not found.**. In **Error! Reference source not found.**, at t=0.42 s, unstiffened parts of the truck fail and the truck becomes unstable. At t= 0.65 s, the front and back tires both slide against the barrier as shown in **Error! Reference source not found.**. At, t=0.76 s, the SUT becomes unstable and leans against the barrier and the body of the truck is observed to slide for a duration of 1.1 s, as seen in **Error! Reference source not found.**. In three consecutive figures, **Error! Reference source not found.**, **Error! Reference source not found.** and **Error! Reference source not found.**, the vehicle can be observed to be in sliding motion with the barrier. The front wheels are projected up in the air while the SUT is being diverted away from the barrier in **Error! Reference source not found.** at 1.22 s. **Error! Reference source not found.** gives the state of vehicle at t=1.31 s, when the wheels return back to the ground and the truck is diverted away from the barrier. At, t=1.52 s, the SUT is directed away from the barrier completely and severe damage is observed as shown in **Error! Reference source not found.**. The simulation comes to an end at t=2.2 s with the SUT completely diverted away from the barrier but with severe damage as seen in Figure 5.25. The barrier can be considered structurally adequate to divert the vehicle safely.

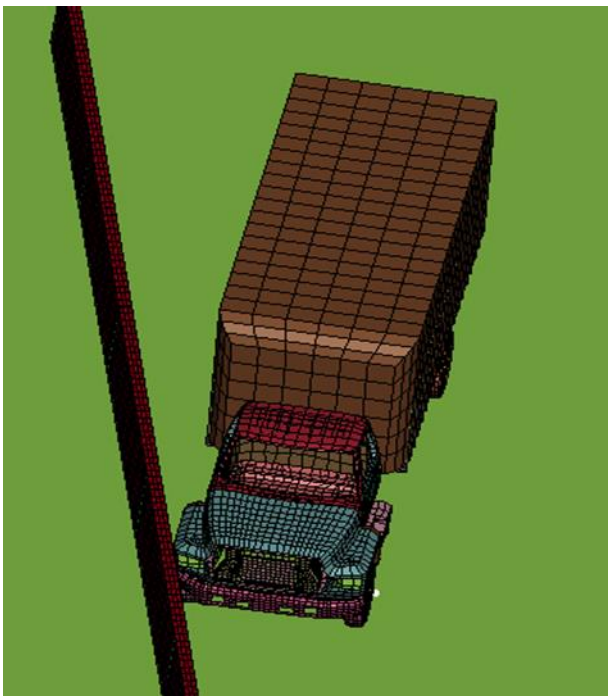

Figure 5.10 At t=0 s, before Impact

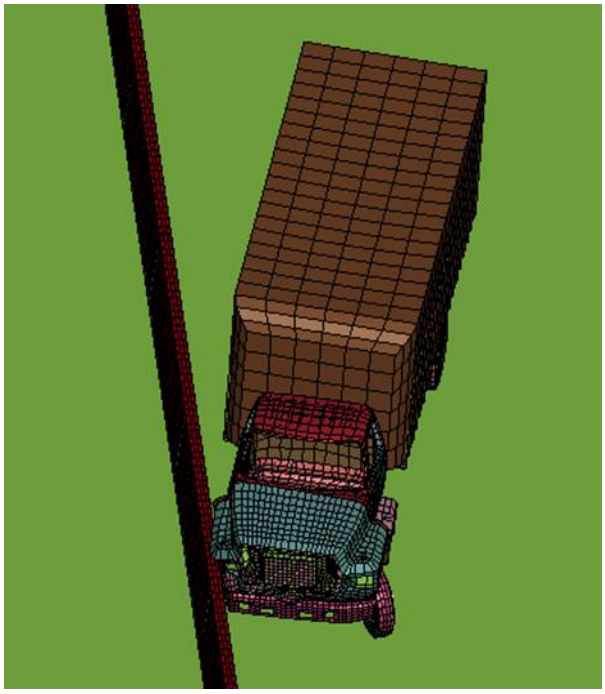

Figure 5.11 At t=0.09 s, Frontal Crush of the Vehicle is Observed

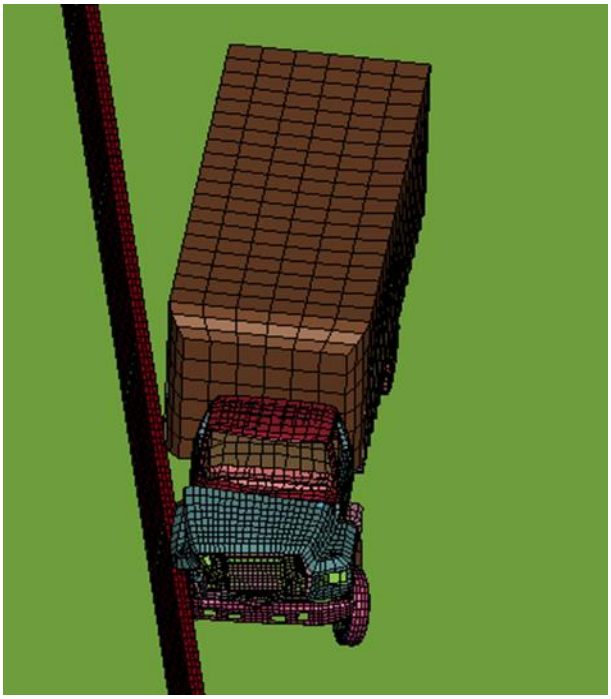

Figure 5.12 At t=0.16 s, the Front Part of Vehicle Starts to Redirect

Figure 5.13 At t=0.2 s, the Trailer Overrides the Barrier

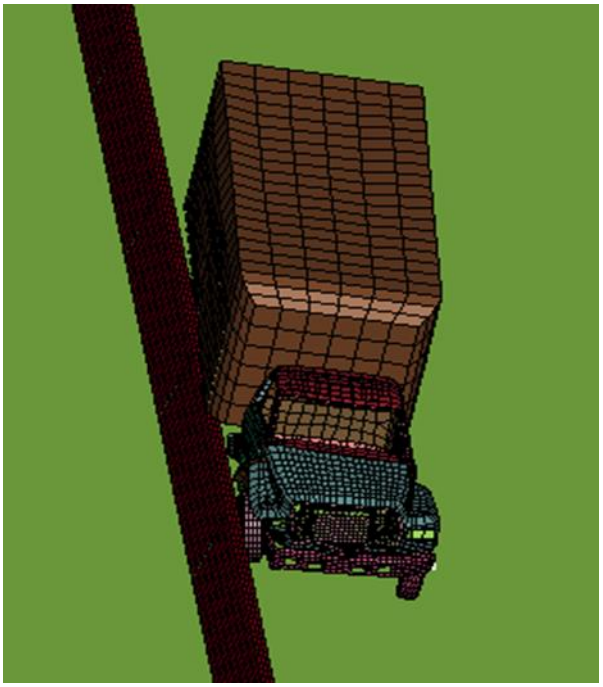

Figure 5.14 At t=0.28 s, the Back Tires Come in Contact with the Barrier

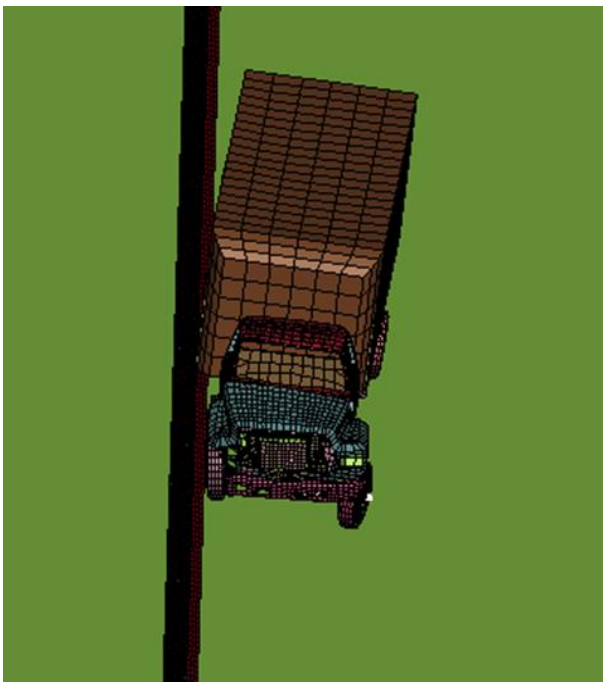

Figure 5.15 At t=0.32 s, the Back Tires Ride the Barrier and Slide against it

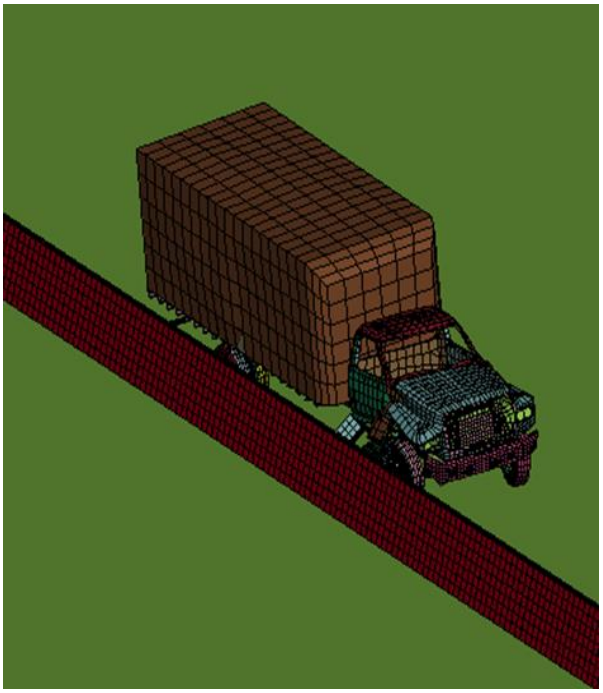

Figure 5.16 At t= 0.42 s, the Unstiffened Parts of Truck Fail and Truck Becomes Unstable

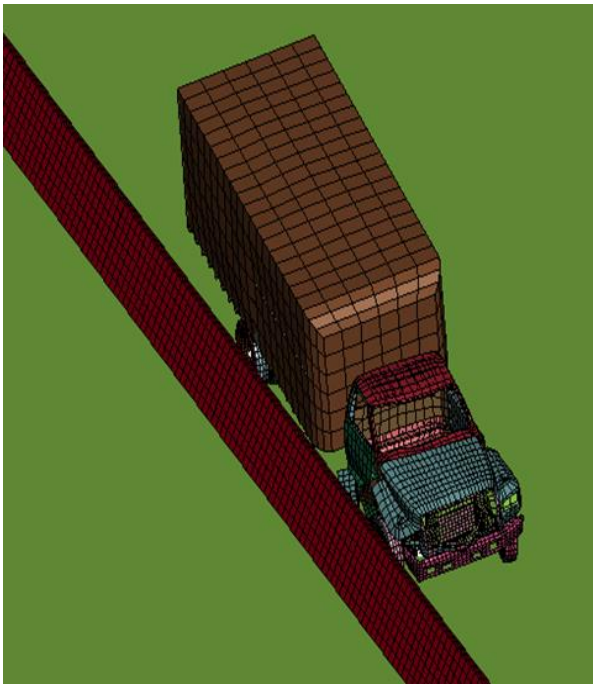

Figure 5.17 At t=0.65 s, Both Front and Back Tires Slide against the Barrier

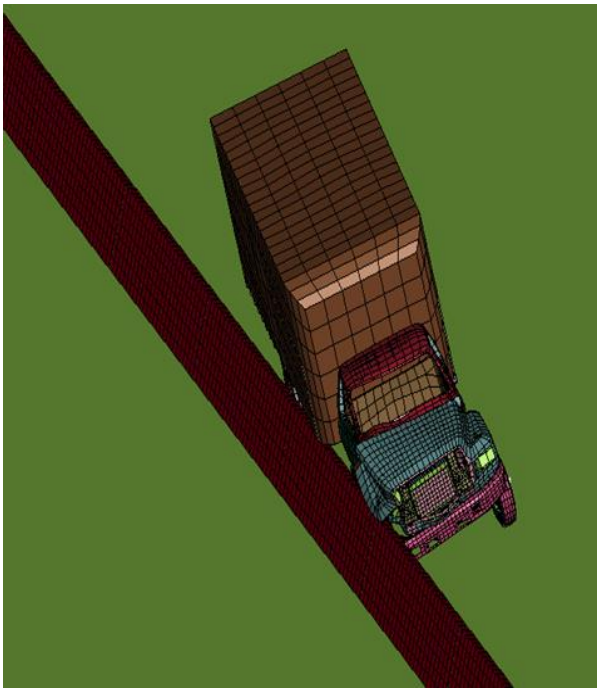

Figure 5.18 At t=0.76 s, the SUT Leans against the Barrier

Figure 5.19 At t=0.81 s, the SUT Body Slides against the Barrier

Figure 5.20 At t=0.95s, the SUT Continues Sliding along the Barrier

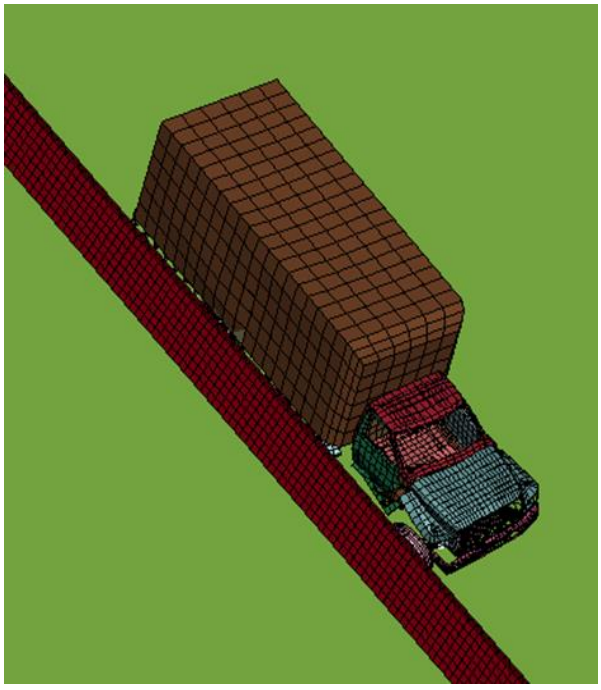

Figure 5.21 At t=1.1s, the SUT Continues Sliding along the Barrier

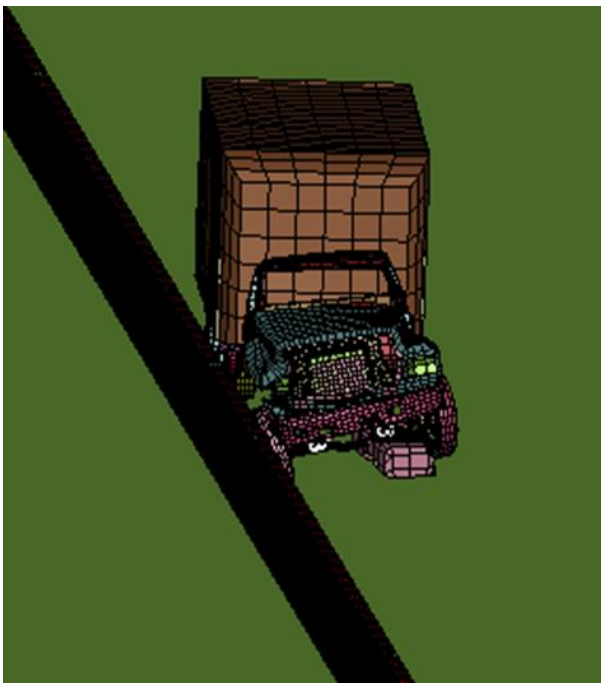

Figure 5.22 At t=1.22 s, the Front Wheels are in the Air while the SUT is Being Directed

Figure 5.23 At t=1.31 s, the Truck is Diverted with Wheels Down

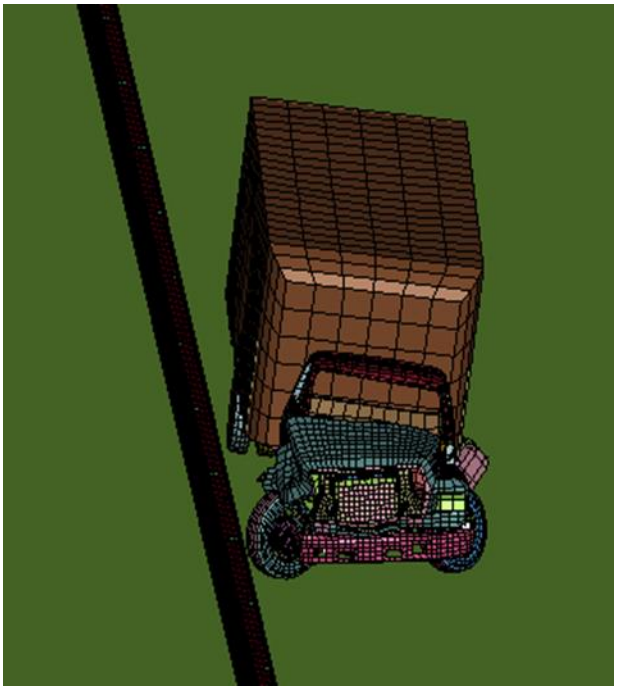

Figure 5.24 At t=1.52 s, the SUT is Directed away from the Barrier Completely; Significant Damage is Observed

Figure 5.25 At t=2.2 s, Simulation Ends

5.6 Occupant Risk Factors

LS-DYNA gives the option to place an accelerometer anywhere on the vehicle to measure different values that can be used to observed different physical characteristics. An accelerometer, as shown in Figure 5.26, is placed in the cabin of the vehicle in order to model occupant risk factors.

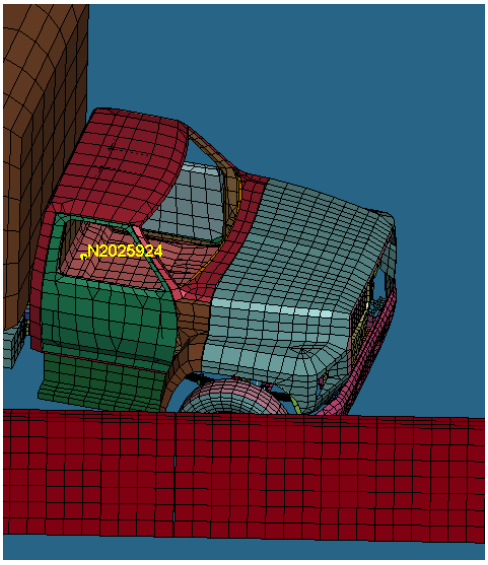

Figure 5.26 Accelerometer Location to Measure Different Risk Factors

*EELEMENT_SEATBELT_ACCELEROMETER is used to select desired nodes as the accelerometer in LS-DYNA. The *DATABASE_ASCII_OPTION keyword card is used to get the desired data from the accelerometer for the certain time interval. In this case, occupant risk factors like roll and pitch rates, which are the rotation of the vehicle in all three directions, are measured. The *DATABASE_ASCII_OPTION_NODOUT card is used to get the rotation of vehicle in X, Y and Z axes, which provides the occupant risk factors. Structural adequacy is the ability of a barrier to successfully divert the crashing vehicle in the same lane without letting it intrude into another lane, whereas the occupant risk factors give the measurement of the injury or severity of accident to the occupant of the vehicle during the crash.

Figure 5.27 and Figure 5.28 give the roll and pitch rates for the SUT measured by the accelerometer placed in the cabin of the truck. In the figure, the y-axis is the relative rotation of the vehicle in the given direction with respect to time. The rotation angles are measured in radians and then converted into degrees to evaluate the criteria in Table 5-1.

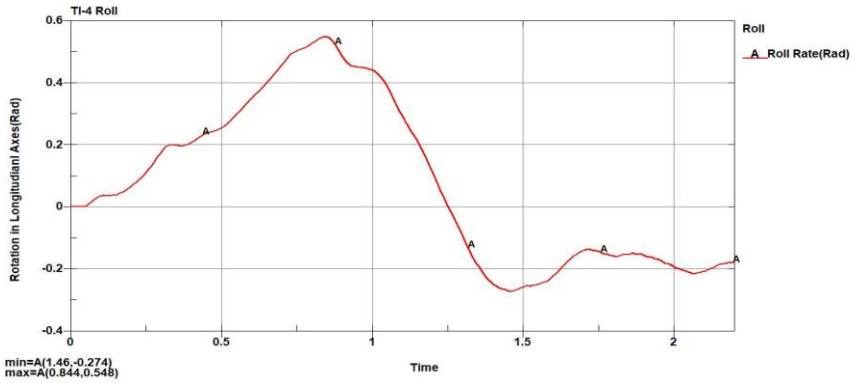

Figure 5.27 TL-4 Roll Rate

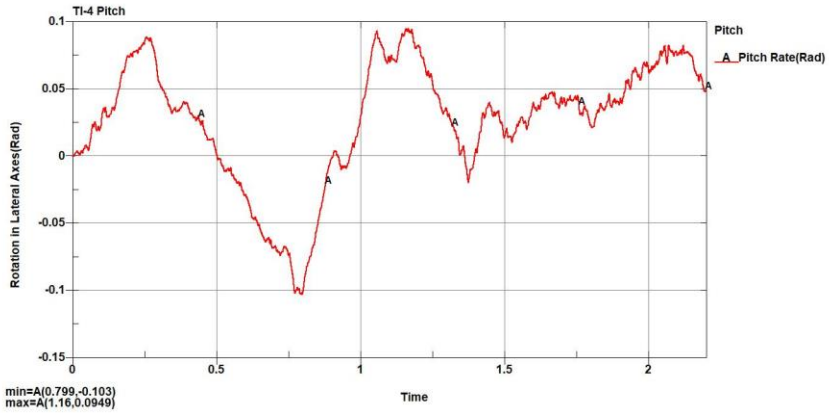

Figure 5.28 TL-4 Pitch Rate

Table 5-1 Occupant Risk Factors Evaluation

Occupant Risk Factors	Max Value (Deg)	Time (s)	Comments
Roll Rate	31.39°	1.46	<75° (Pass)
Pitch Rate	-5.9°	0.8	<75° (Pass)

5.7 Overturning Stability and Structural Damage of TL-4 Barrier

After the full-scale crash simulation of the 40-ft (12.2 m) long TL-4 barrier, small overturning moment is observed in the barrier. The bottom edge of the impact face is displaced 0.127 in (3.23 mm) in the vertical direction in the striking face of the barrier. The concrete from the barrier failed at the top of the barrier where the truck and its trailer came in contact with the barrier (Figure 5.29). The displacement caused by the moment is shown in Figure 5.30. The barrier section at the point of impact had maximum permanent deflection of 1.5 in (39.1 mm) in the horizontal direction, which was measured by taking a node of concrete section at the top of the barrier. Similarly, the maximum permanent deflection of the longitudinal reinforcement obtained by taking a node in the beam section was 1.35 in (34.3 mm).

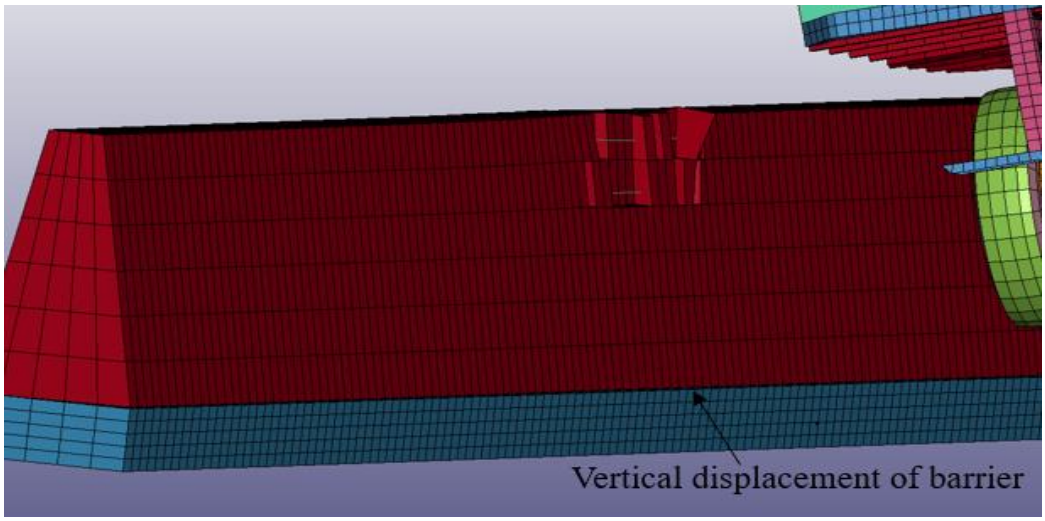

Figure 5.29 Damage of 42-in Barrier

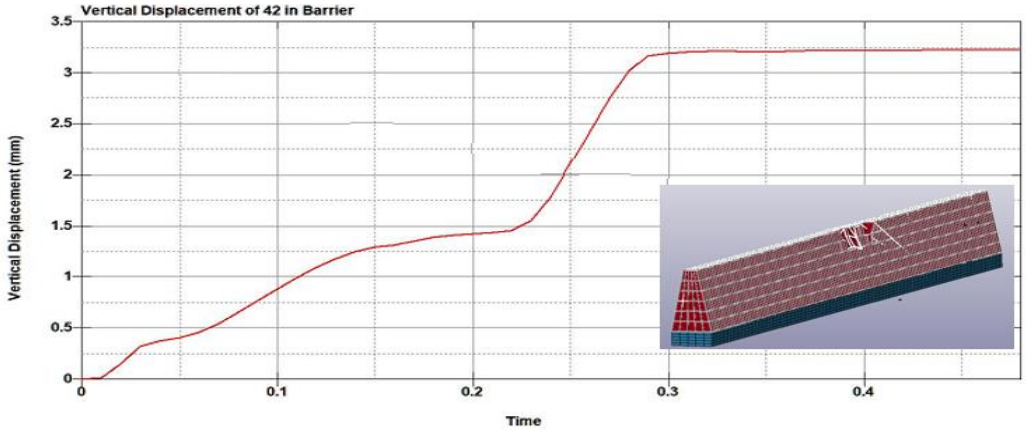

Figure 5.30 Displacement of Barrier

5.8 Summary: MASH TL-4 Evaluation Criteria for UDOT 42-in Barrier

Table 5-2 represents the evaluation criteria for 42-in (1067 mm) constant slope barrier subject to MASH TL-4. Satisfactory results are obtained for both the evaluation factors and criteria that are analyzed in this report. The vehicle is observed to be diverted safely and does not override or underride the installation. It is damaged in a predictable manner by concrete at the point of impact. Thus, the barrier passes Criteria A, B and C of the MASH evaluation for structural adequacy. Similarly, the vehicle remained upright during and after the collision and the maximum angles did not exceed 75°. Thus, the barrier passes Criteria F of the MASH evaluation for occupant risk factors.

Table 5-2 MASH TL-4 Evaluation Criteria for UDOT 42 in barrier

Factor	Criteria	Result	Comments
Structural Adequacy	A	Satisfactory - Pass	Vehicle is diverted in a safe manner, although damage to the vehicle is observed
	B	Satisfactory - Pass	The test barrier activated in a predictable manner by fracturing
	C	Satisfactory - Pass	The test barrier redirected and controlled vehicle; penetration was not allowed
Occupant Risk	F	Satisfactory - Pass	Vehicle remained in upright direction with acceptable roll and pitch rates observed

6. TL-5 MASH EVALUATION OF UDOT 54-INCH CONSTANT SLOPE BARRIER

6.1 FEM of 54-in Barrier

The cross-section view of the 54-in barrier FEM is shown in Figure 6.1. The isometric view of the barrier is shown in Figure 6.2. Each section of the barrier is 12-ft (3.66 m) long with a 10-in (254 mm) expansion joint provided at the end of each barrier. The same modeling procedures and steps as presented in Section 5.1 of this report are applied in modeling the 54-in barrier. Similar to TL-4, TL-5 barrier evaluation is also conducted in two phases. The average size of the null shell and solid shell element is 7.87 in (200 mm).

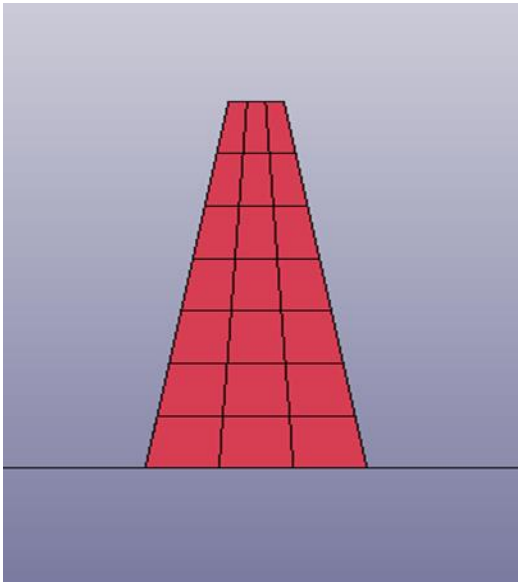

Figure 6.1 Cross-Section View of 54-in (1372 mm) Barrier

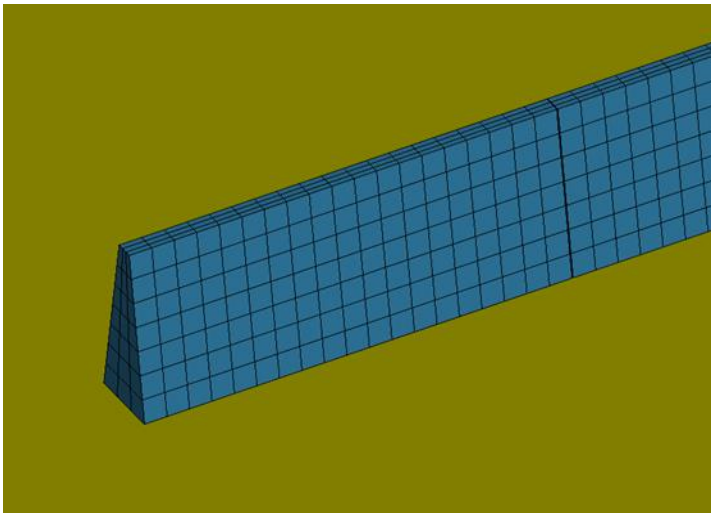

Figure 6.2 Isometric View of 54-in (1372 mm) Barrier

Figure 6.3 represents the FEM of full-scale concrete barrier and base. Figure 6.4 represents the dowel bars in the PCCP base. Figure 6.5 represents the longitudinal and dowel reinforcement for the TL-5 barrier. Stirrups are not modeled in the TL-5 barrier to save computation time in simulation.

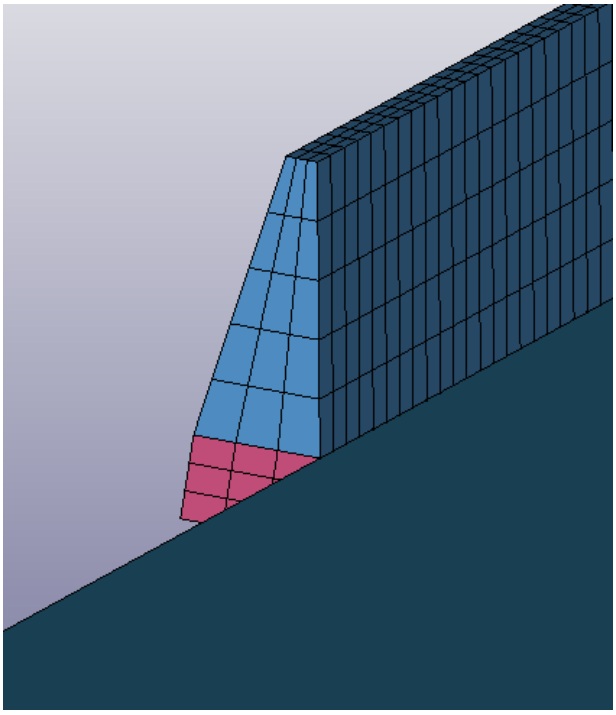

Figure 6.3 FEM of Barrier, Base and Ground

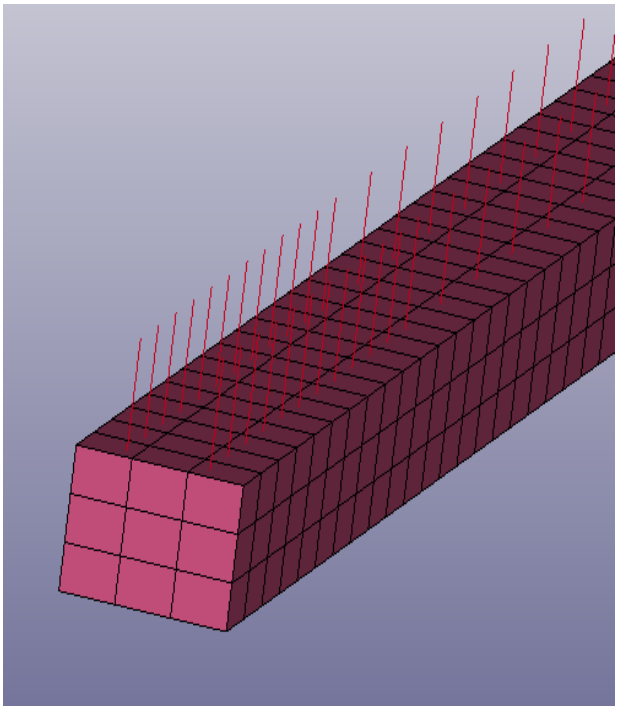

Figure 6.4 FEM of Dowel Bars in PCCP Base

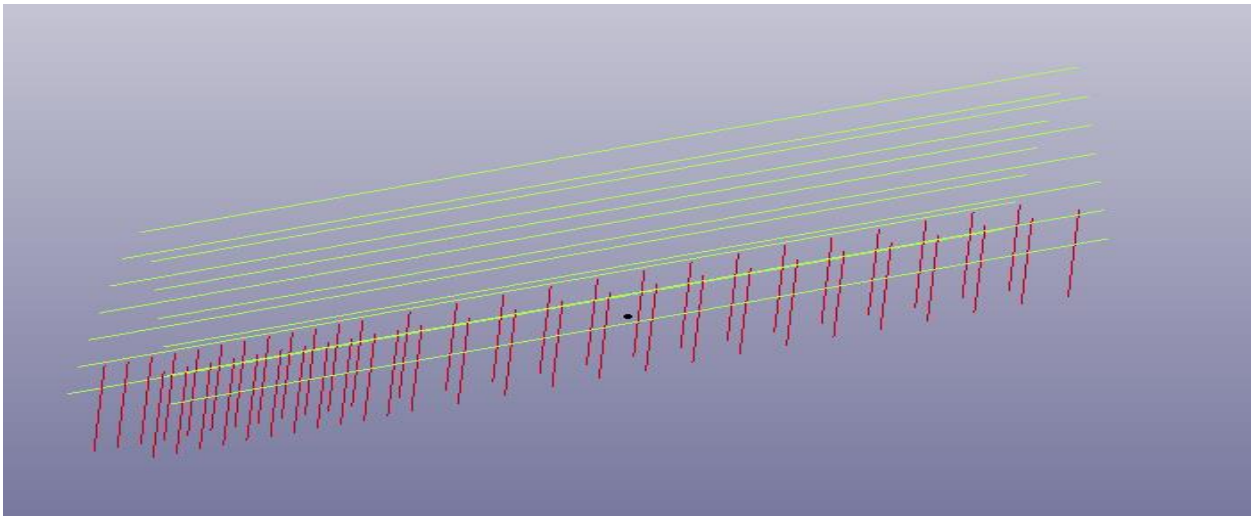

Figure 6.5 FEM of 54-in (1372 mm) Barrier Reinforcement

6.2 FEM of Tractor-Trailer

The tractor-trailer (TL-5) model was originally developed by the NCAC at GWU. Improvements were made by ORNL and the University of Tennessee at Knoxville. Among the models of tractor available, the sleeper-cab tractor is selected for the simulation along with the 48-ft (14.63 m) long trailer. The sleeper-cabin tractor (Figure 6.6) has a 249-in (6325 mm) wheel base and is 8.23 tons in weight. It consists of 115816 elements and 459 unique parts.

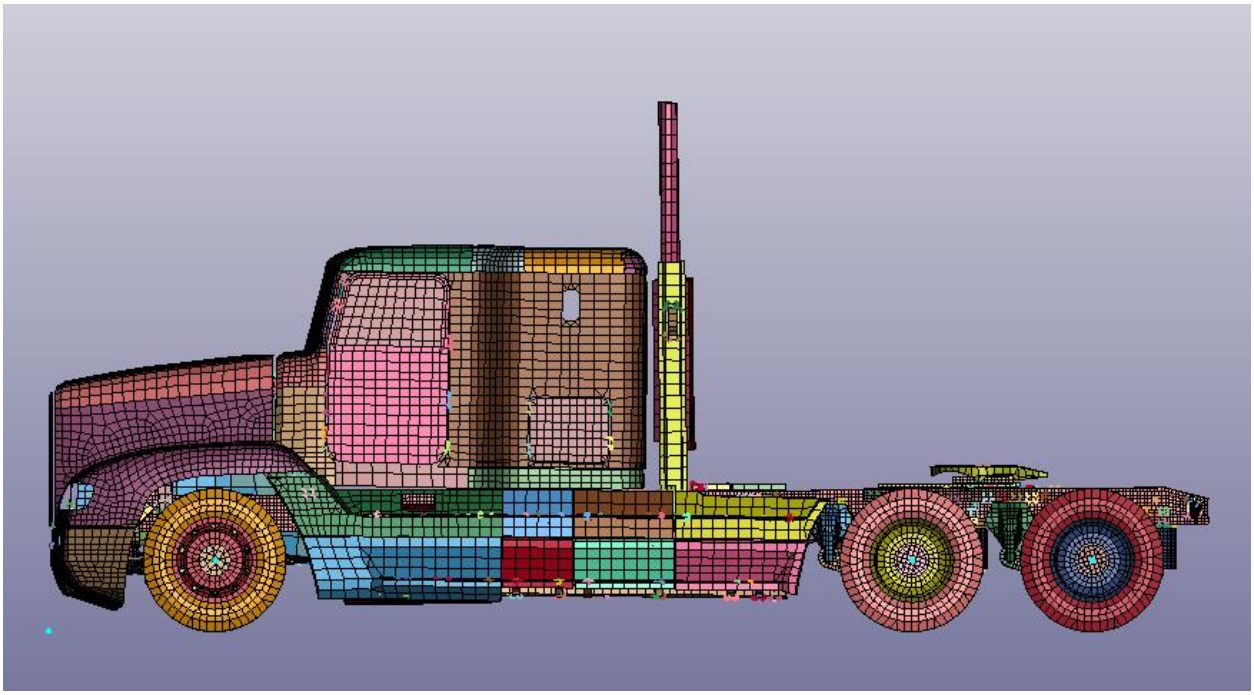

Figure 6.6 Sleeper-Cab Tractor FEM

The trailer (Figure 6.7) has 246226 elements and 104 parts and measures 6.27 tons in weight. The kingpin in the trailer is inserted into the fifth wheel of the tractor to connect the tractor to trailer to form the whole tractor-trailer model (Figure 6.8).

Figure 6.9 shows the tractor, trailer and the load assembled together, as the MASH TL-5 test vehicle. The tractor and trailer are joined through the fifth mechanical wheel and kingpin using CONSTRAINED_JOINT _ SPHERICAL where the kingpin moves around the fifth mechanical as a spherical joint but does not disconnect (**Error! Reference source not found.** and **Error! Reference source not found.**). Since, MASH TL-5 recommends using a 36-ton vehicle, a load of 21.4 tons is added to the trailer to achieve the load limit. The load is fixed in the trailer bed using TIED_NODES_TO_SURFACE_OFFSET.

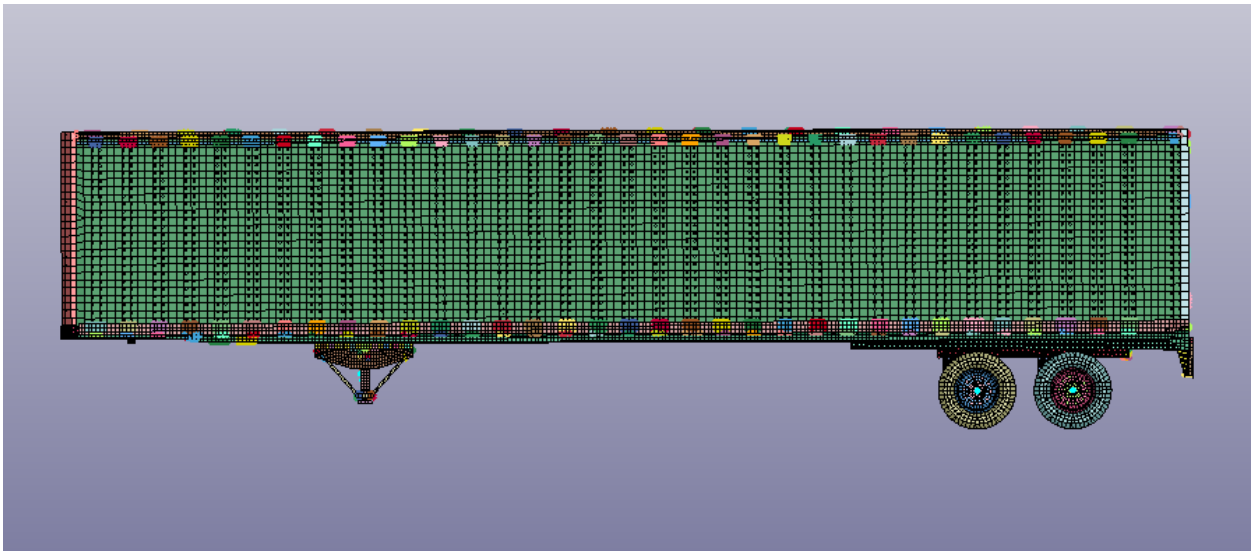

Figure 6.7 Trailer FEM

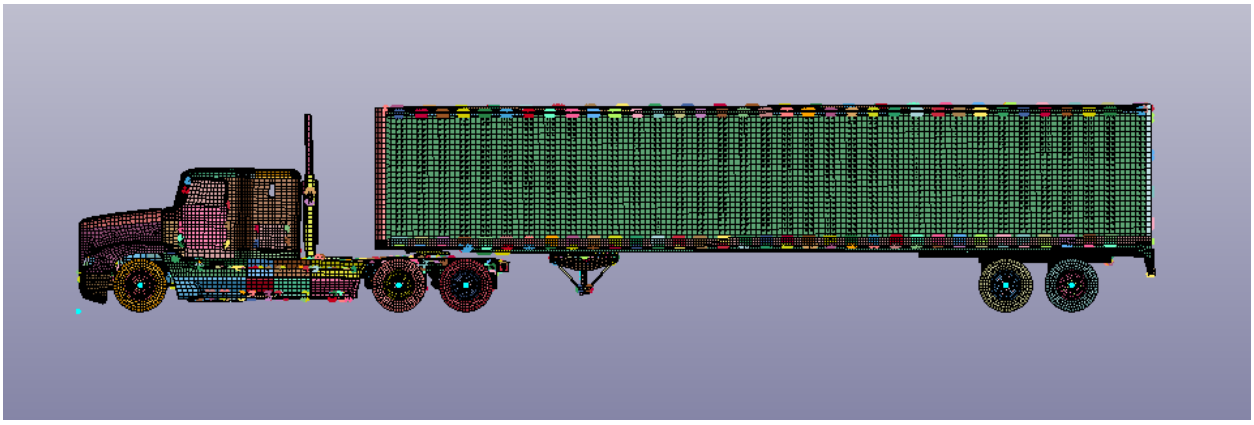

Figure 6.8 Full FEM of Tractor-Trailer

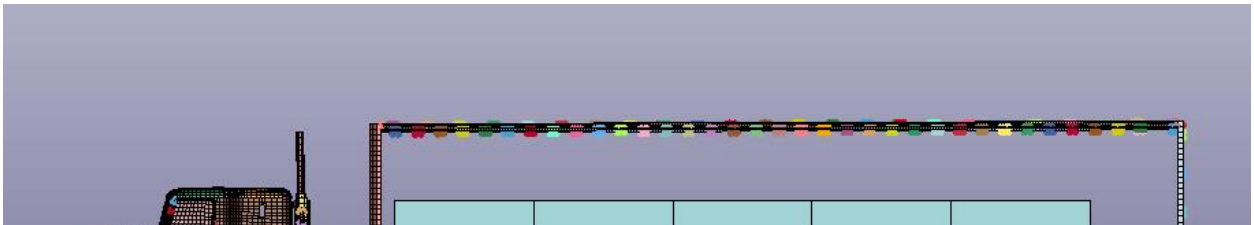

Figure 6.9 Tractor, Trailer and Load Together

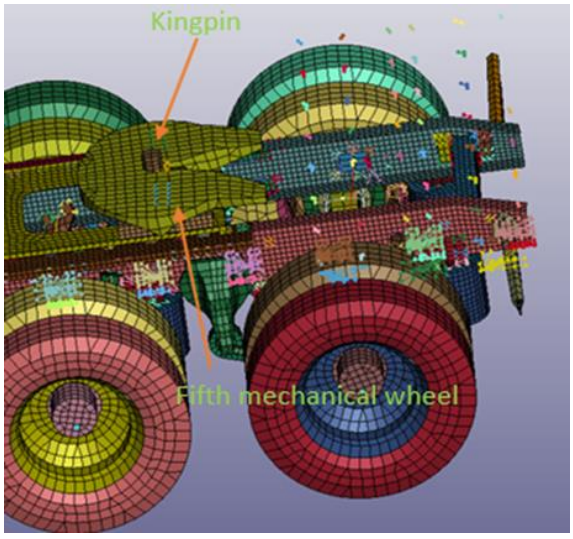

Figure 6.10 Joint Between Fifth Mechanical Wheel and Kingpin

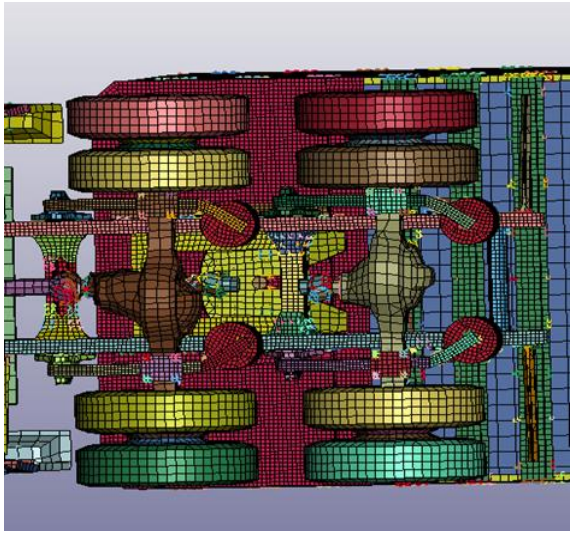

Figure 6.11 Connection Between Tractor and Trailer

6.3 Validity of TL-5 Model

The energy balance equation for the simulation of 54-in (1372 mm) barrier with a MASH TL-5 test vehicle is shown in Figure 6.12. The total energy is taken as constant, while the decrease in kinetic energy and summation of increase in internal energy and sliding energy is equivalent. Hourglass energy is determined to be negligible. Thus, the simulation can be considered valid, since the total energy is conserved.

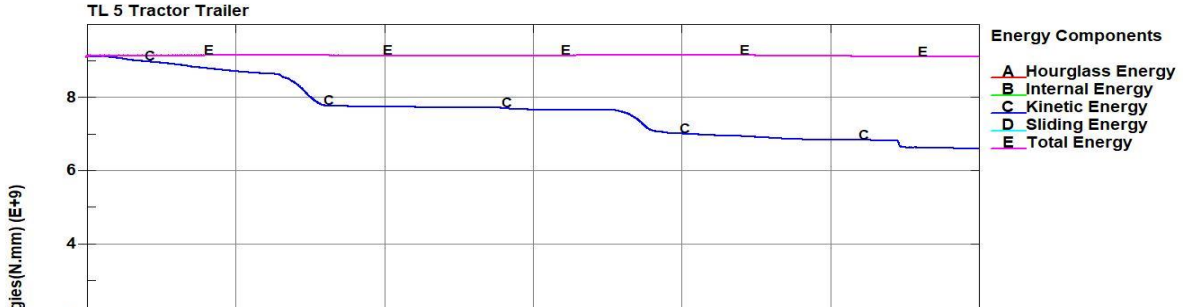

Figure 6.12 Energy Balance Equation for Simulation of TL-5 54-inch Barrier

6.4 TL-5 Crash Simulation Time History Description

The crash simulation is illustrated in the subsequent figures of this section. The figures show the different state of the tractor-trailer during the crash simulation. Figure 6.13 shows the tractor-trailer at the state just before crash. Figure 6.14 shows the initial crush of the frontal part of the tractor-trailer at t=0.07 s after the start of the simulation. In Figure 6.15, the tractor part of the tractor-trailer begins to redirect away from the barrier. The trailer comes in contact with the barrier after 0.29 s of the simulation, which is seen in Figure 6.16. As seen in Figure 6.17, redirection of the trailer after the impact is observed. In Figure 6.18 the tractor-trailer is diverted away from the barrier. The rear part of the tractor-trailer comes in contact with the barrier at 0.75 s as shown in Figure 6.19. In Figure 6.20, the trailer is observed to slide with the barrier. Figure 6.21 shows the trailer being diverted away from the barrier and at t=1.03 s, the front part of the trailer is in contact with the barrier again as seen in Figure 6.22. Finally, in Figure 6.23, at 1.2 s, the tractor is observed to divert away from the barrier completely.

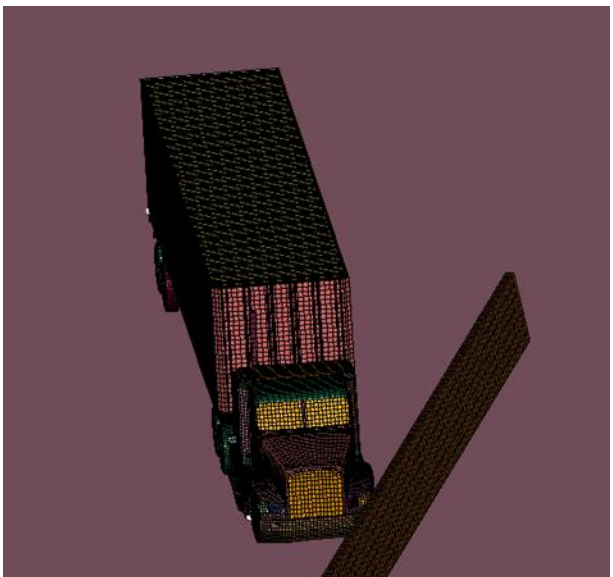

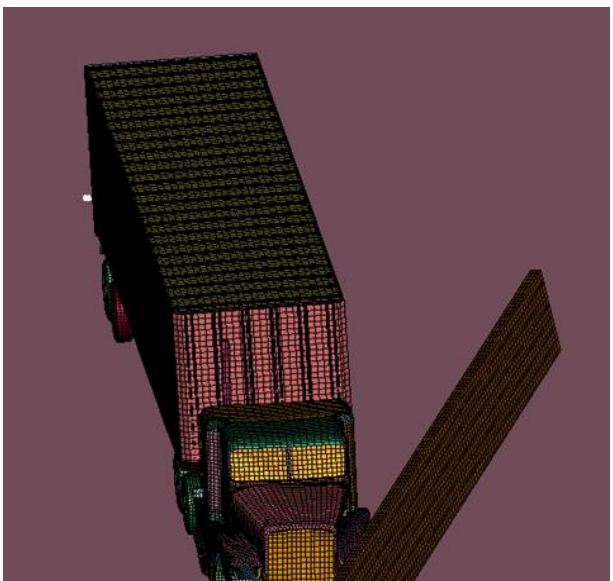

Figure 6.14 At t=0 s, Prior to Impact

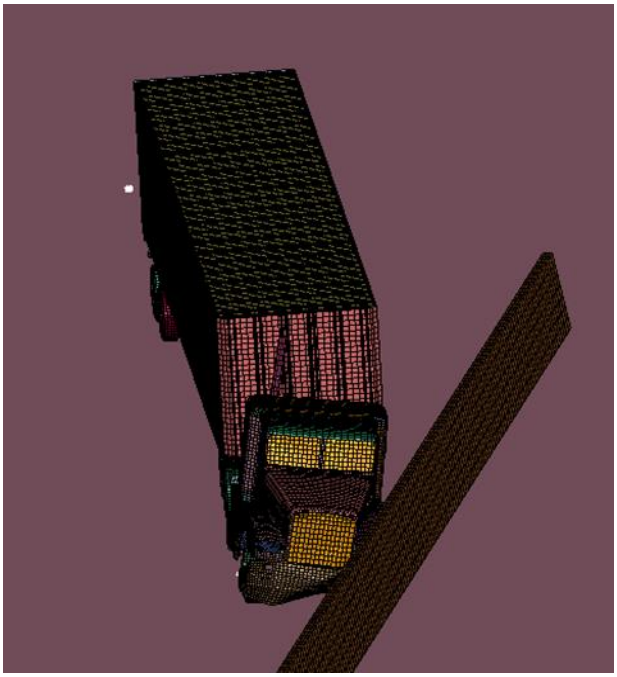

Figure 6.15 At t=0.13 s, after Impact the Tractor Starts to Redirect

Figure 6.16 At t= 0.29 s, Contact between the Trailer and Barrier

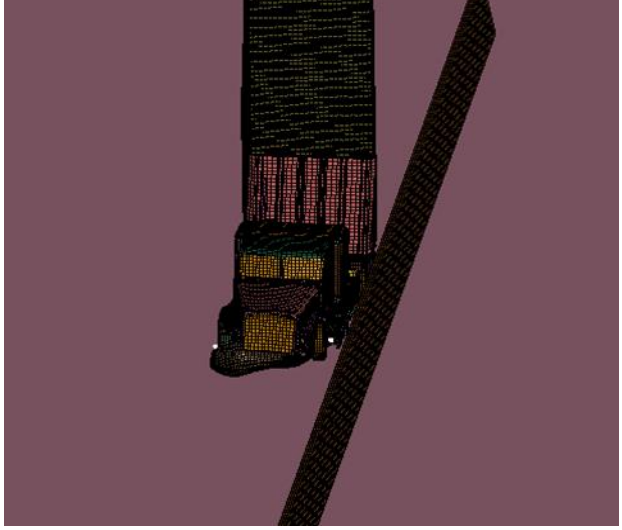

Figure 6.18 At t= 0.52 s, after Impact, No Contact with the Barrier

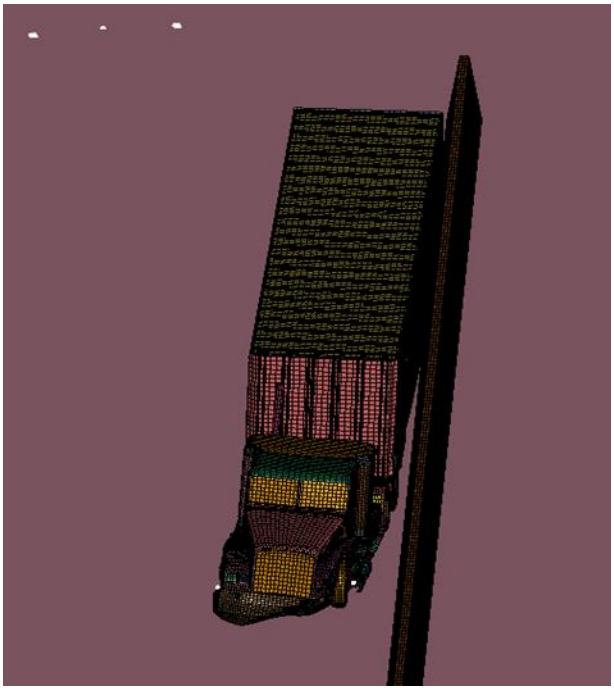

Figure 6.19 At t=0.75 s, Contact of Rear Part of Trailer with Barrier

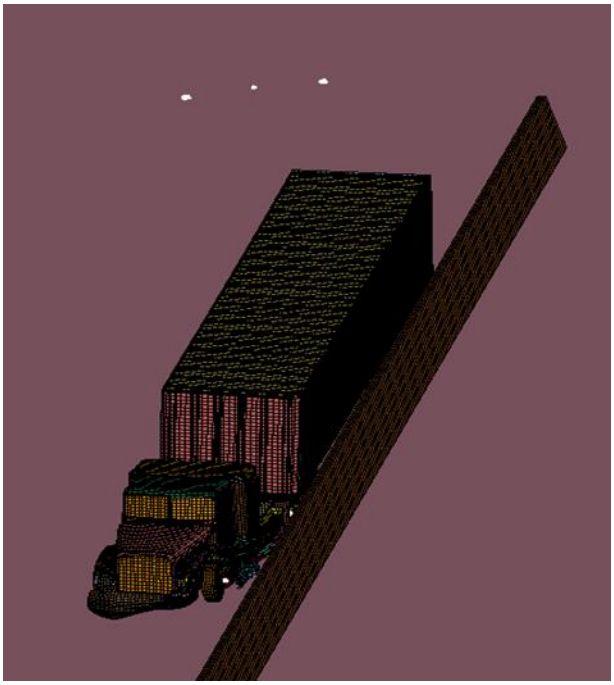

Figure 6.20 At t=0.83 s, Trailer Comes in Contact and Slides Along Barrier

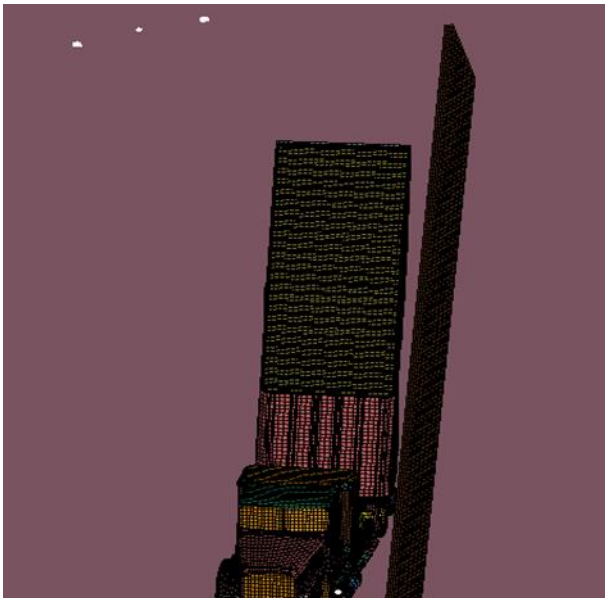

Figure 6.22 At t=1.03 s, Front Part of Trailer Comes in Contact again with Barrier

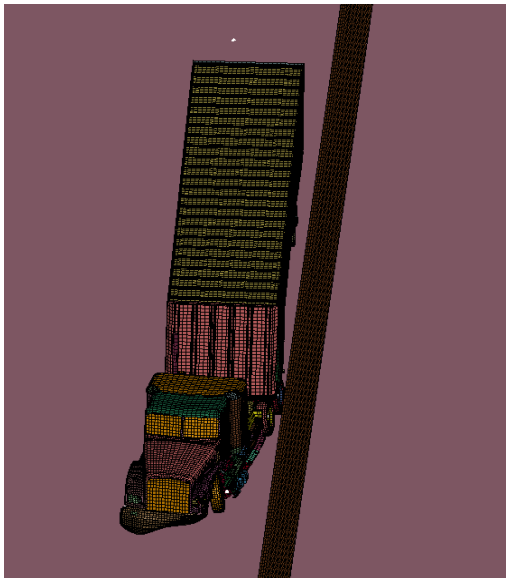

Figure 6.23 At t=1.2 s, Tractor-Trailer is Completely Diverted from the Barrier

6.5 Occupant Risk Factors

An accelerometer (Figure 6.24) is mounted in the tractor to measure the rotation of the tractor in all three axes. The measurements give the occupant risk factors of roll and pitch rates. More explanation of the procedures for extracting the occupant risk factors from the accelerometer is provided in Section 5.6 of this report. The roll and pitch rates are the rotation of the vehicle in three different axes. LS-DYNA gives the time history of the rotation of the

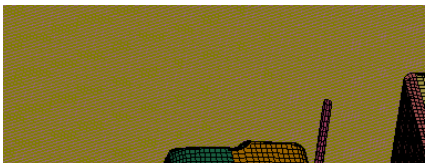

accelerometer in radians. The maximum value is converted to degrees and compared with the MASH requirements to analyze the occupant risk factors associated with the barrier.

Figure 6.24 Accelerometer Mounted in Tractor

The rotation angles are measured in radians and then converted into degrees to evaluate the criteria in **Error! Reference source not found.**. The values in Table 6-1 are maximum values obtained during the simulation. Figure 6.25 and Figure 6.26 give the roll and pitch rate, respectively, for the tractor- trailer measured by the accelerometer placed in the cabin of the truck. In the figures, the y-axis is the relative rotation of the vehicle in the given direction with respect to time.

Table 6-1 Occupant Risk Factors Evaluation

Occupant Risk Factors	Value (Deg)	Time (s)	Comments
Roll Rate	34.37°	0.35	<75 °(Pass)
Pitch Rate	-11.45°	0.3	<75 °(Pass)

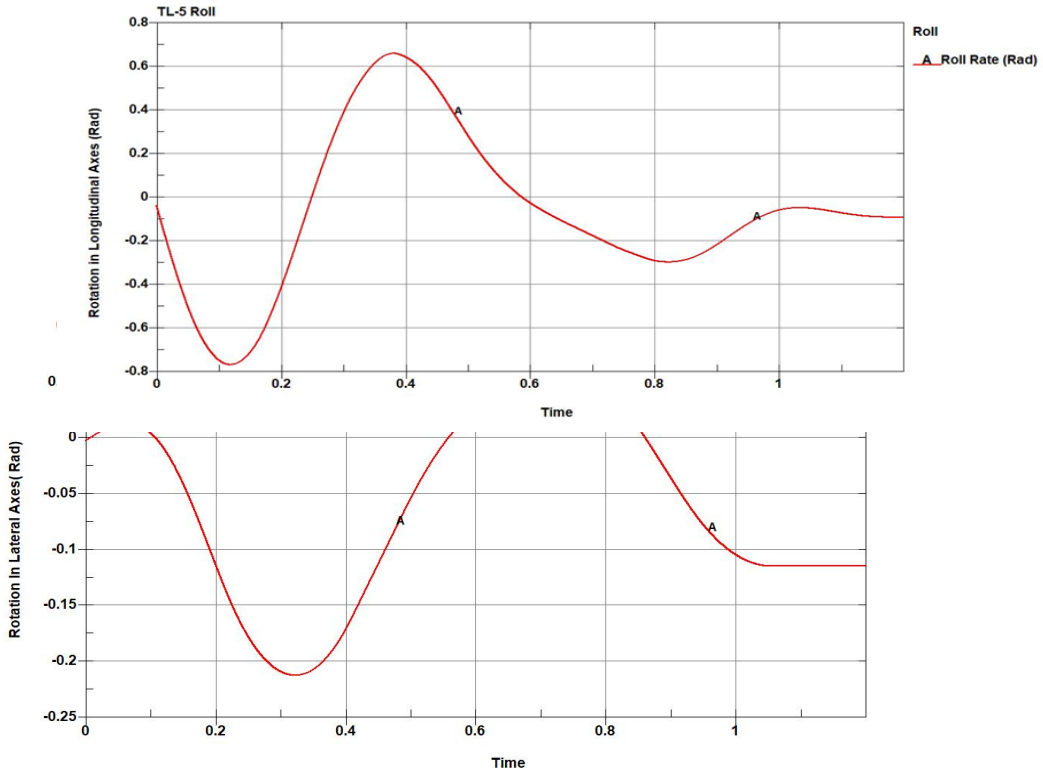

Figure 6.26 TL-5 Pitch Rate

6.6 Overturning Stability and Structural Damage of TL-5 Barrier

In the case of full-scale TL-5 barrier, the simulation of 0.33 s is constrained due to the computing limitations. In this section, only the results from 0.33 s long simulation are discussed. The full-scale crash simulation is carried out on 80-ft (24.38 m) long TL-5 barrier (Figure 6.27 and Figure 6.28).

Crushing of concrete and deformation of reinforcement can be seen in Figure 6.29 and Figure 6.30. Figure 6.31 gives the horizontal displacement of a reference node, which is

observed to be about 2.4 in (63 mm). The vertical displacement of the barrier section caused by the overturning moment is observed to be 0.01 in (0.33 mm) (Figure 6.32). Through the simulation it can be observed that although concrete damage is significant at the top of the barrier where the trailer contacts it, the barrier is safe against the overturning moment. However, longer time simulation can provide better results.

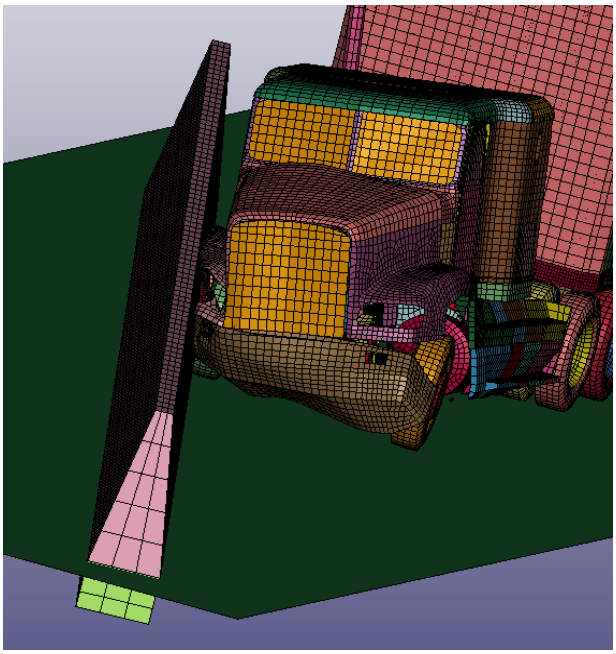

Figure 6.27 At t=0.11s Tractor Comes in Contact with the Barrier

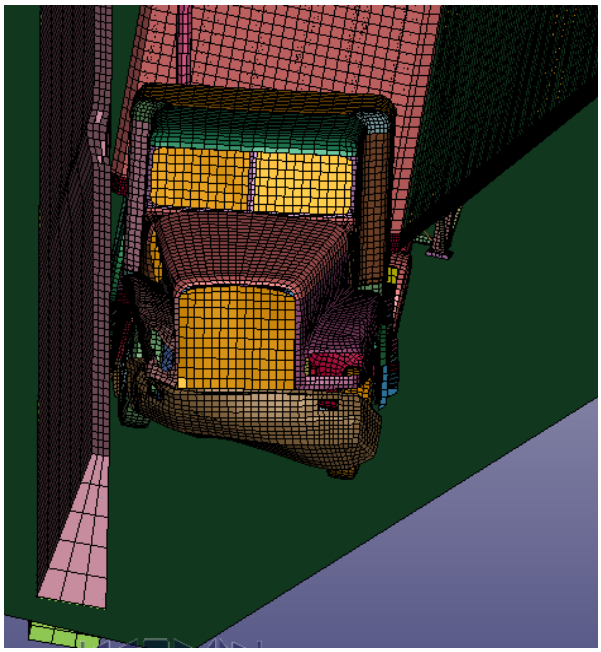

Figure 6.28 At t=0.33 s Trailer is Rebounded from the Barrier

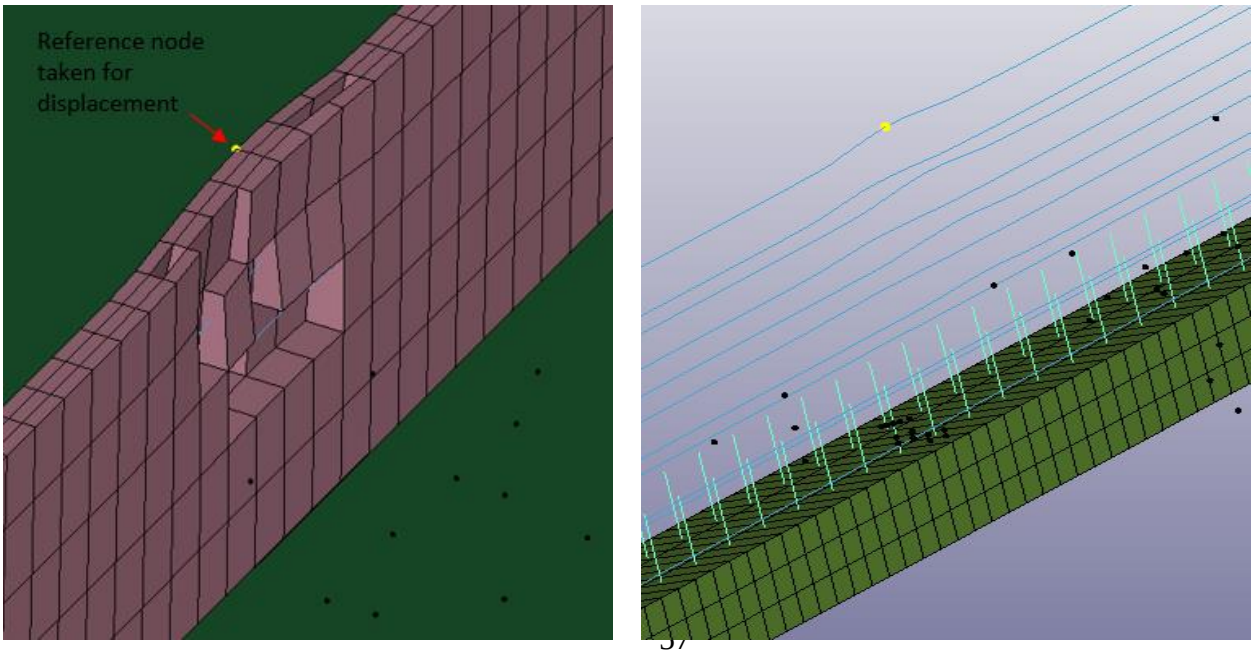

Figure 6.29 Damage of Concrete Elements

Figure 6.30 Damage in Reinforcement Elements

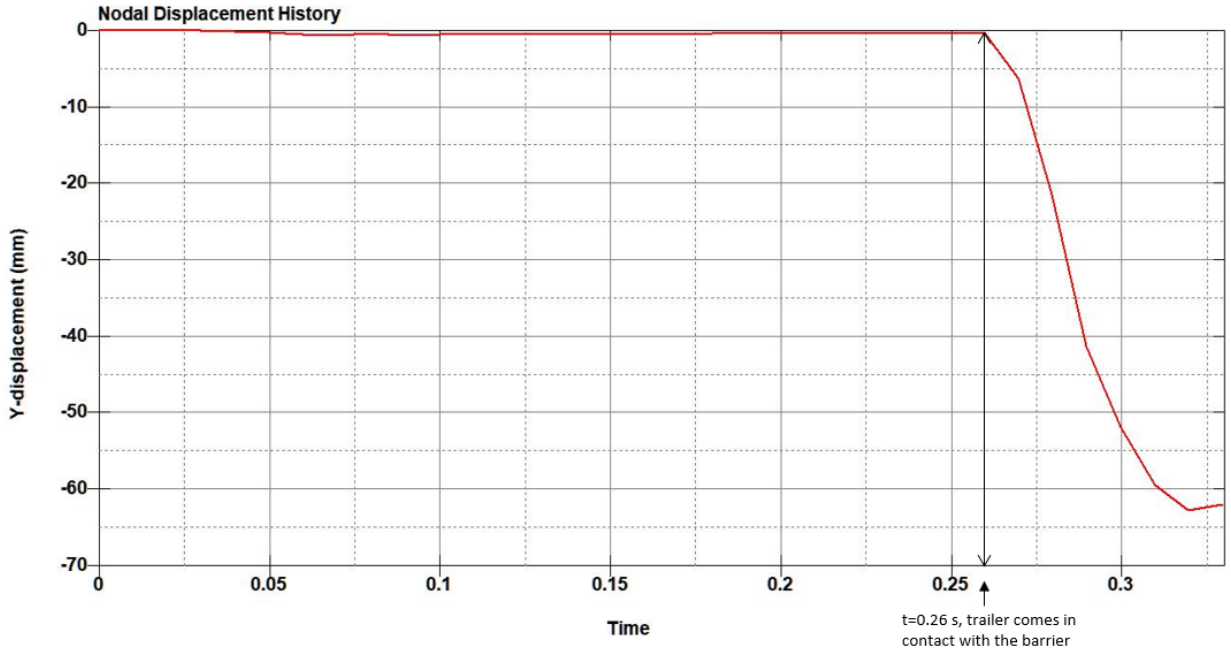

Figure 6.31 Nodal Displacement History of Concrete Node

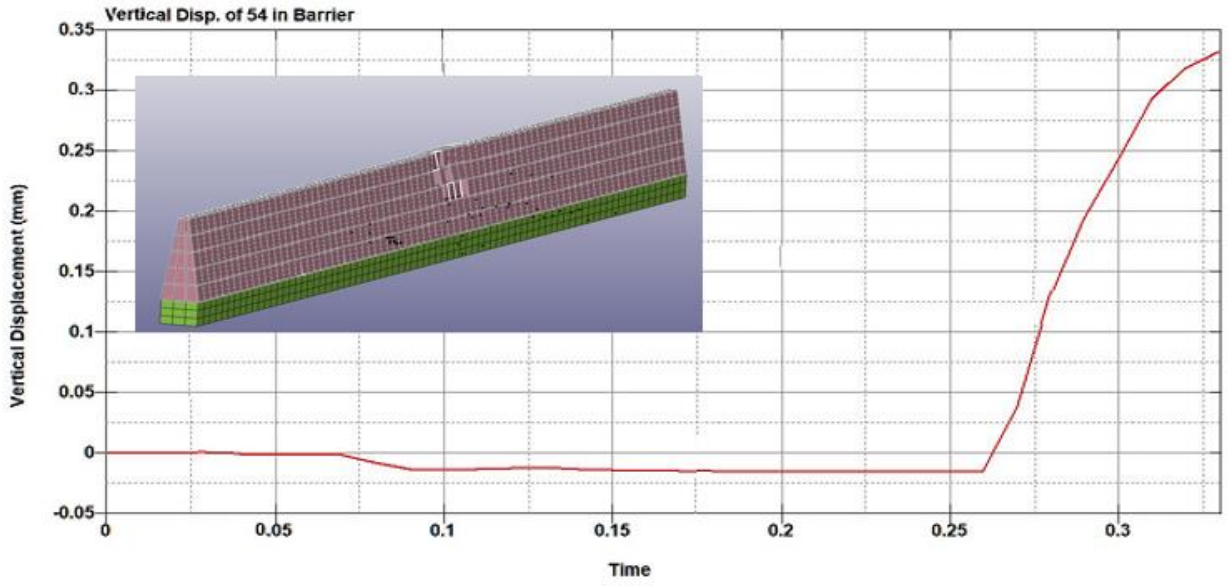

Figure 6.32 Vertical Displacement of Barrier

6.7 Summary: MASH TL-5 Evaluation Criteria for UDOT 54-in Barrier

Table 6-2 represents the evaluation criteria for 54-in constant slope barrier subject to MASH TL-5 impact conditions. Satisfactory results are obtained for both the evaluation factors and criteria that are analyzed in this report. The vehicle is observed to be diverted safely and it does not override or underride the installation. Thus, the barrier passes Criteria A and B of the MASH evaluation for structural adequacy. Criteria C could not be analyzed due to shorter duration of simulation. Similarly, the vehicle remained upright during and after the collision and the maximum angles did not exceed 75°. Thus, the barrier passes Criteria F of the MASH evaluation for occupant risk factor.

Table 6-2 MASH TL-5 Evaluation Criteria for UDOT 54 in Barrier

Factor	Criteria	Result	Comments
Structural Adequacy	A	Satisfactory - Pass	Vehicle is diverted in a safe manner, although damage to the vehicle is observed
	B	Satisfactory – Pass	The test barrier activated in a predictable manner by deflecting
Occupant Risk	F	Satisfactory - Pass	Vehicle remained in upright direction with acceptable roll, and pitch rate observed

7. RESULTS AND CONCLUSION

The finite element modeling and simulation using LS-DYNA provides satisfactory results for structural adequacy for MGS barrier when tested for MASH TL-3. Both occupant risk factors and structural adequacy are obtained for the 42-in (1067 mm) constant slope barrier when tested for MASH TL-4 impact conditions, and the 54-in (1372 mm) constant slope barrier when tested for MASH TL-5 impact conditions. The flexible MGS barrier is able to reduce the speed of the crashing vehicle and redirect it while sustaining large deflection in the barrier section. In the case of rigid TL-4 and TL-5 barriers, the vehicle is diverted into the same lane without overriding the barrier although permanent damage to the barrier and vehicles is observed.

Thus, it can be concluded that the MGS, 42-in (1067 mm) and 54-in (1372 mm) constant slope barriers are safe and fulfil their functionality according to FHWA MASH standards when analyzed using FEM software LS-DYNA.

REFERENCES

Abraham, N., Ghosh, B., Simms, C., Thomson, R., & Amato, G. (2016). Assessment of the impact speed and angle conditions for the EN1317 barrier tests. *International Journal of Crashworthiness*, *21*(3), 211–221. https://doi.org/10.1080/13588265.2016.1164444

Albin, R. B., Bullard, D. L., Abu-odeh, A., & Menges, W. L. (2002). *Washington State Precast Concrete Barrier*.

American Association of State Highway and Transportation Officials. (2016). *Manual for Assessing Safety Hardware, 2016.* (Second).

Atahan, A. O. (2006). Finite-Element Crash Test Simulation of New York Portable Concrete Barrier with I-Shaped Connector. *Journal of Structural Engineering*, *132*(March 2006), 322–324. https://doi.org/10.1061/(ASCE)0733-9445(2006)132

Atahan, A. O. (2009). Effect of permanent jersey-shaped concrete barrier height on heavy vehicle post-impact stability. *International Journal of Heavy Vehicle Systems*, *16*(1–2), 243–257. https://doi.org/10.1504/IJHVS.2009.023863

Bielenberg, B.W., Faller, R.K., Rohde, J.R., Reid, J.D., Sicking, D.L., and Holloway, J. H. (2007). *Development of Tie-Down and Transition Systems for Temporary Concrete Barrier on Asphalt Road*.

Bligh, R. P., Sheikh, N. M., Alberson, D. C., & Abu-Odeh, A. Y. (2006). Low-deflection portable concrete barrier. *Transportation Research Record*, (1984), 47–55. https://doi.org/10.3141/1984-07

Borovinšek, M., Vesenjak, M., Ulbin, M., & Ren, Z. (2007). Simulation of crash tests for high containment levels of road safety barriers. *Engineering Failure Analysis*, *14*(8 SPEC. ISS.), 1711–1718. https://doi.org/10.1016/j.engfailanal.2006.11.068

Consolazio, G. R., Chung, J. H., & Gurley, K. R. (2003). Impact simulation and full scale crash testing of a low profile concrete work zone barrier. *Computers and Structures*, *81*(13), 1359–1374. https://doi.org/10.1016/S0045-7949(03)00058-0

Crash Simulation Vehicle Models | NHTSA. (n.d.). Retrieved March 11, 2020, from https://www.nhtsa.gov/crash-simulation-vehicle-models

Dhafer Marzougui, G. B., & Eskandarian, A. (2004). *Evaluation of Portable Concrete Barriers Using Finite Element Simulation (No. NCAC 2002-W-001)*. The National Crash Analysis Center.

Esfahani, E. S., & Opiela, K. S. (2008). *Safety Performance of Concrete Median Barriers under Updated Crashworthiness Criteria(N0. NCAC 2008-W002)* (No. NCAC 2008-W-002). The National Crash Analysis Center.

F800 SUT Model. (2005). Retrieved March 11, 2020, from https://thyme.ornl.gov/FHWA/F800WebPage/simulations/simulations.html

Faller, R. K., Polivka, K. A., Kuipers, B. D., Bielenberg, R. W., Reid, J. D., Rohde, J. R., & Sicking, D. L. (2004). Midwest Guardrail System for Standard and Special Applications. *Transportation Research Record: Journal of the Transportation Research Board*, *1890*(1), 19–33. https://doi.org/10.3141/1890-03

Hourglass — Welcome to the LS-DYNA support site. (2020). Retrieved March 11, 2020, from https://www.dynasupport.com/howtos/element/hourglass

Itoh, Y., Liu, C., & Kusama, R. (2007a). Dynamic simulation of collisions of heavy high-speed trucks with concrete barriers. *Chaos, Solitons and Fractals*, *34*(4), 1239–1244. https://doi.org/10.1016/j.chaos.2006.05.059

Itoh, Y., Liu, C., & Kusama, R. (2007b). Modeling and simulation of collisions of heavy trucks with concrete barriers. *Journal of Transportation Engineering*, *133*(8), 462–468. https://doi.org/10.1061/(ASCE)0733-947X(2007)133:8(462)

KA, P., FK, F., DL, S., JR, R., BW, B., JD, R., & BA, C. (2006). *Performance Evaluation of the Permanent New Jersey Safety Shape Barrier. Update to NCHRP 350 Test NO. 4-12 (2214NJ-2)*.

Kevin Schrum, Dean Sicking, N. U. (2016). *Evaluation of Design Loads for Concrete Bridge Rails*.

Kim, W., Lee, I., Jeong, Y., Zi, G., Kim, K., & Lee, J. (2018). Design Approach for Improving Current Concrete Median Barriers on Highways in South Korea. *Journal of Performance of Constructed Facilities*, *32*(3), 1–10. https://doi.org/10.1061/(ASCE)CF.1943-5509.0001168

Lee, E., Shrivatri, A., & Ohara, S. (2017). NHTSA Oblique Test Data Analysis Method by LS-DYNA Modeling. *25th International Technical Conference on the Enhanced Safety of Vehicles (ESV)*, 17–0243.

LSTC. (2012). *LS-DYNA KEYWORD USER'S MANUAL VOLUME II Material Models*.

Marzougui, D, Kan, C. D., & Opiela, K. S. (2014). Crash Test & Simulation Comparisons of a Pickup Truck & a Small Car Oblique Impacts Into a Concrete Barrier. *13th International*

LS-DYNA Users Conference, 1–18.

Marzougui, Dhafer, Buyuk, M., & Kan, S. (2007). *PERFORMANCE EVALUATION OF PORTABLE CONCRETE BARRIERS*. Contract No. DTFH61-02-X-00076.

Marzougui, Dhafer, Kan, C. D., & Opiela, K. (2012). Comparison of crash test and simulation results for impact of Silverado pickup into New Jersey barrier under manual for assessing safety hardware. *Transportation Research Record*, *14*(2309), 114–126. https://doi.org/10.3141/2309-12

Michie, J. D. (1993). Recommended Procedures for the Safety Performance Evaluation of Highway Appurtenances. In *National Cooperative Highway Research Program Report 350*.

Millar, C. W. W., & Authority, P. (1993). National Cooperative Highway Research Program NCHRP Report 350 Safety Performance Evaluation. In *National Cooperative Highway Research Program Report 350*.

Procedures for Verification and Validation of Computer Simulations Used for Roadside Safety Applications(2011). (2011). In *National Academies of Sciences, Engineering, and Medicine 2011*. https://doi.org/10.17226/17647

Reid, J. D. (2009). Approach slopes for midwest guardrail system. *Journal of Transportation Safety and Security*, *1*(1), 32–45. https://doi.org/10.1080/19439960902735212

Reid, J. D., Kuipers, B. D., Sicking, D. L., & Faller, R. K. (2009). Impact performance of W-beam guardrail installed at various flare rates. *International Journal of Impact Engineering*, *36*(3), 476–485. https://doi.org/10.1016/j.ijimpeng.2008.08.006

Sheikh, N. M., Bligh, R. P., & Fossier, P. (2014). Pinned-down temporary concrete barrier with transition systems for limited-space work zone applications. *Transportation Research Record*, *2437*, 78–88. https://doi.org/10.3141/2437-08

Sicking, D. L., Reid, J. D., & Rohde, J. R. (2002). Development of the Midwest Guardrail System: *Https://Doi.Org/10.3141/1797-06*, (1797), 44–52. https://doi.org/10.3141/1797-06

Trajkovski, J., Ambrož, M., & Kunc, R. (2018). The importance of friction coefficient between vehicle tyres and concrete safety barrier to vehicle rollover - FE analysis study. *Journal of Mechanical Engineering*, *64*(12), 753–762. https://doi.org/10.5545/sv-jme.2018.5290

Wang, Q., Fang, H., & Yin, H. (2018). A probability-based approach for assessment of concrete median barriers. *International Conference on Transportation and Development 2018: Connected and Autonomous Vehicles and Transportation Safety - Selected Papers from the*

International Conference on Transportation and Development 2018, 171–179. https://doi.org/10.1061/9780784481530.017

Wang, S., Lei, Z., Zhao, J., Lei, M., Li, Y., & Liu, Y. (2011). A research of similarity design of collision guardrails under the overpass. *2011 2nd International Conference on Mechanic Automation and Control Engineering, MACE 2011 - Proceedings*, 1903–1906. https://doi.org/10.1109/MACE.2011.5987337

Yin, H., Fang, H., Wang, Q., & Wen, G. (2016). Design optimization of a MASH TL-3 concrete barrier using RBF-based metamodels and nonlinear finite element simulations. *Engineering Structures*, *114*(April 2019), 122–134. https://doi.org/10.1016/j.engstruct.2016.02.009

Yonten, K., Manzari, M. T., Marzouqui, D., & Eskandarian, A. (2005). An assessment of constitutive models of concrete in the crashworthiness simulation of roadside safety structures. *International Journal of Crashworthiness*, *10*(1), 5–19. https://doi.org/10.1533/ijcr.2005.0321